HIGH THROUGHPUT ASSESSMENT OF KINASE INHIBITORS IN SACCHAROMYCES CEREVISIAE IDENTIFIES ANEUGENIC COMPOUNDS

by
Vivian Yeong

A thesis submitted to Johns Hopkins University in conformity with the requirements for the degree of Master of Science in Engineering

Baltimore, Maryland

April 2017

Abstract

Most solid tumors are comprised of cells with abnormal numbers of chromosomes, which result from chromosomal missegregation during mitosis. The increased rate of chromosome gains or losses is known as chromosomal instability (CIN) and may be implicated in early tumor development processes. Consequently, there has been significant interest in targeting CIN as a novel therapeutic intervention, especially since increased missegregation may impart drug sensitivity in cancer cells. To discover novel chemical modulators of faithful chromosome segregation, we employed a quantitative chromosome transmission fidelity (qCTF) assay previously used in a genetic screen for CIN phenotypes in *Saccharomyces cerevisiae* and adapted it for a high throughput screen of 418 commercially-available kinase inhibitors. We generated a qCTF strain with increased drug sensitivity and weakened mitotic checkpoint in order to achieve sensitive and cost-effective detection of increases in CIN at minimal inhibitor concentrations. Using the adapted qCTF assay, we developed a pipeline for hit identification, false positive exclusion through additional phenotypic validation assays, and hit verification by colony sectoring assay. 4 of the 418 kinase inhibitors were identified as compounds that significantly increased CIN and target the MAPK pathway, cell cycle regulation, and glycolysis in mammalian cells. Interestingly, our screen identified dabrafenib, an FDA-approved compound used to treat metastatic melanoma, as a potential aneugen. Yeast homologs of the mammalian targets were determined and deleted to identify possible drug targets in yeast. We proposed that HOG1, a key regulator of the hyperosmotic stress response, and BMH1, an isoform of the 14-3-3 family of proteins, may play roles in maintaining chromosome transmission fidelity.

Altogether, this study establishes a high throughput pipeline that can be extended to larger compound libraries to identify drugs that elevate chromosome missegregation and cause lethal aneuploidy.

Advisor: Rong Li **Reader:** Petr Kalab

Acknowledgements

I would like to thank Professor Rong Li for the opportunity to work in her lab, her extensive mentorship, and academic guidance. I thank Jin Zhu for training me to work with yeast, to handle large libraries, to design experiments, and to become an independent and critical thinker. His patience, understanding, and optimism have helped me overcome several challenges in both my research and academic goals. I would also like to thank the Rong Li lab members and reader, Professor Petr Kalab, for creating a welcoming lab environment and for their inputs on my project. Finally, I'd like to thank my loving and supportive parents and brother who have encouraged me to follow my interests, whether they take me half-way across the world in Singapore or just a few hours south of home.

Table of Contents

Abstract ..... **ii**
Acknowledgements ..... **iv**
Table of Contents ..... **v**
List of Tables ..... **vi**
List of Figures ..... **vii**
Chapter 1: Introduction **1**
Chromosomal instability in cancer 1
Mechanisms of chromosomal missegregation 2
The Spindle Assembly Checkpoint (SAC) ensures faithful chromosome segregation 6
Measuring chromosomal instability in yeast 8
Yeast as a model organism 12
Motivation and summary 13
Chapter 2: Materials & Methods **14**
Chemical transformations in yeast 14
Yeast drop test 14
High throughput kinase inhibitor screen procedure 15
Flow cytometry data collection 16
Calculating minichromosome loss rate 16
High throughput screen data analysis 17
Cell sorting and auxotrophic growth assay 17
PI staining 18
Colony sectoring assay 18
Chapter 3: Results and Discussion **20**
Adapting the qCTF assay for a high throughput screen 20
Identifying hits from a primary screen 24
Identifying and excluding false positive hits 26
Validation of top hits using a classical qCTF assay 34
Elucidating novel pathways that contribute to CIN in budding yeast 36
Chapter 4: Conclusions **43**
Summary 43
Future directions 43
Bibliography **45**
Curriculum vitae **50**

List of Tables

Table 2.1: Strains used in this study *15*

Table 3.1: Top 10 putative kinase inhibitors hits that elevate CIN, their pathways, targets and drug color *27*

Table 3.2: The four kinase inhibitor hits, their mammalian targets and pathways . *32*

Table 3.3: Potential drug targets in yeast *37*

List of Figures

Figure 1.1: Mechanisms of chromosomal missegregation 5

Figure 1.2: The spindle assembly checkpoint 7

Figure 1.3: The classical chromosome transmission fidelity 9

Figure 1.4: The qCTF assay detects minichromosome loss 10

Figure 1.5: The qCTF assay demonstrates sensitive detection of changes in CIN and a large dynamic range 12

Figure 3.1: Homozygous deletion of genes regulating membrane permeability and efflux pumps increases drug sensitivity 22

Figure 3.2: Heterozygous deletion of MAD2 weakens the mitotic checkpoint and increases basal CIN rate in yeast 23

Figure 3.4: The distribution of pathways targeted by the top 20 kinase inhibitors . 25

Figure 3.5: Abnormal GFP profiles were observed in some treated samples 26

Figure 3.6: Unidentified populations are comprised of dead cells 28

Figure 3.7: PI staining reveals that the unidentified population is comprised of dead cells stained with drug 29

Figure 3.8: 24 kinase inhibitors reduce cell proliferation 31

Figure 3.9: The remaining kinase inhibitor hits that increase CIN by more than 5-fold 32

Figure 3.10: Colony sectoring assay verifies top four kinase inhibitor hits 35

Figure 3.11: Heterozygous and homozygous deletions of MAPK components. 39

Figure 3.12: YLR345W is not required for proper chromosome segregation. 41

Figure 3.13: CIN of heterozygous IPL1 deletion mutant treated with aurora A kinase inhibitor 42

Chapter 1: Introduction

Normal cellular function is dependent on the equal division of genetic material between two daughter cells. Failure to do so can have detrimental consequences, often resulting in diseases such as Down's syndrome and cancer. This chapter reviews how chromosomal instability is implicated in cancer, the mechanisms by which errors in chromosome partitioning arise, a robust surveillance mechanism that detects and guards against chromosome missegregation, assays used to measure chromosomal instability, and yeast as a model organism for the high throughput study of modulators of chromosomal segregation.

Chromosomal instability in cancer

70-90% of human tumors are comprised of cells with abnormal numbers of chromosomes, which results from chromosomal missegregation during mitosis (Weaver & Cleveland, 2006; Kops, Weaver, & Cleveland, 2005). This loss or gain of whole chromosomes at increased rates is known as chromosomal instability (CIN) and has been implicated in early tumor development processes (Bakhoum & Compton, Chromosomal instability and cancer: a complex relationship with therapeutic potential, 2012). As a result, there has been significant interest in targeting CIN for novel therapeutic interventions, especially since increased missegregation rates have been shown to impart drug sensitivity in tumor cells and may even suppress tumor formation above some threshold CIN level (Janssen, Kops, & Medema, 2009). Moreover, whole chromosome missegregation can generate a diverse cell population, which contributes to the adaptability and evolvability of cancer cells

especially under selection pressures (Cahill, Kinzler, Vogelstein, & Lengauer, 199). The intratumor heterogeneity that results from CIN produces cells with a diverse set of genotypes, some of which may confer a selective advantage. These advantageous mutations allow a small population of cells to overcome selection pressures and ultimately result in the propagation of a clonal population that can proliferate even in the presence of the selection. However, too much chromosomal instability results in the massive loss of essential genes required for cell survival, and consequently, cells that demonstrate excessive CIN produce progeny that are highly aneugenic and often inviable. Recently, there has been increasing interest in exploiting CIN as a potential cancer therapeutic. Current developing therapeutics attempt to target specific mediators of chromosome segregation that are speculated to elicit a more pronounced effect in cancer cells, including Aurora B, which destabilizes MT-KT attachments, HSET, which maintains proper spindle polarity, and components in the autophagy pathway (Tanaka & Hirota, 2016). These therapeutics take advantage of the already defective chromosome segregation mechanisms present in cancer cells and further aggravate them in order to arrest the cell and induce apoptosis.

Mechanisms of chromosomal missegregation

There are four primary routes of chromosomal missegregation that occur during mitosis – defects in mitotic checkpoint, sister chromatid cohesion, microtubule-kinetochore attachments, and centrosome amplification. After cells have duplicated their genetic content, their chromosomes condense and line up in a single plane during metaphase. Spindle microtubules emanating from opposite poles then form the proper attachments to

kinetochores of both sister chromatids, and pull the chromatids apart. The cell undergoes cytokinesis, generating two daughter cells with equal partitioning of genetic material. Defects in several steps during mitosis can interfere with the faithful division of chromosomes.

The mitotic checkpoint, also known as the spindle assembly checkpoint (SAC), senses the presence of unattached kinetochores and responds by delaying anaphase (Holland & Cleveland, 2009). More specifically, the SAC halts mitotic progression by sequestering the E3 ubiquitin ligase, anaphase promoting complex/cyclosome (APC/C), and prevents it from interacting with downstream mitotic substrates such as cell cycle regulators and securin (Kops, Weaver, & Cleveland, 2005). A compromised mitotic checkpoint results in premature entry into anaphase in spite of improper microtubule-kinetochore attachments or chromosomal misalignments. As a result, sister chromatids may fail to separate and be inherited together, generating a daughter cell that is aneuploid (Figure 1.1).

Defects in sister chromatid cohesion is an additional contributor to chromosomal missegregation. Cohesin is a protein that holds sister chromatids together until they are pulled towards the spindle poles during anaphase (Kops, Weaver, & Cleveland, 2005). During anaphase, cohesin is cleaved by separase, which is inhibited and sequestered by securin in metaphase (Kops, Weaver, & Cleveland, 2005). Abnormalities in cohesin degradation can cause sister chromatids to fail to separate during anaphase, resulting in aneuploid daughters. Similarly, chromosomal missegregation may also result from premature sister chromatid separation (Figure 1.1). Sister chromatid cohesion defects have been implicated in various cancers exhibiting chromosomal instability, including

Hodgkin's lymphoma and human colorectal cancers (Sajesh, 2013; Barber, 2008). Furthermore, a study that sequenced 102 human genes related to yeast CIN genes identified 11 somatic mutations in colorectal cancer, 10 of which play direct roles in sister chromatid cohesion (Barber, 2008).

Another mechanism that affects the faithful partitioning of chromosomes is the establishment of faulty attachments of kinetochores to spindle microtubules. More specifically, merotelically attached kinetochores – single kinetochores that are attached to spindles from both poles – are undetected by the SAC because sufficient tension is generated by the microtubule-kinetochore attachments (Kops, Weaver, & Cleveland, 2005). Since MT-KT attachments are dynamic and constantly undergo disassociation and reassociation, errors in MT-KT attachment are often resolved (Thompson, Bakhoum, & Compton, 2010). However, failure to correct merotelic attachments results in lagging chromosomes, which may be inherited by a single daughter cell or become lost from both daughter nuclei and form individual micronuclei (Figure 1.1) (Kops, Weaver, & Cleveland, 2005). Interestingly, in colorectal cancer cell lines, lagging chromatids were observed in the majority of cells exhibiting mitotic defects and high percentages of lagging chromatids have been found in breast, colon, and lung tumors (Thompson S. L., 2008). Regulation of KT-MT dynamics may present a therapeutic opportunity as exemplified by one study, which reported that overexpression of kinesins that promote MT-KT destabilization rescue chromosome missegregation phenotypes in tumor cell lines exhibiting increased CIN (Bakhoum, Thompson, Manning, & Compton, 2009).

The final pathway to chromosome missegregation discussed in this chapter is centrosome overamplification. Normal cell division occurs in a bipolar orientation with

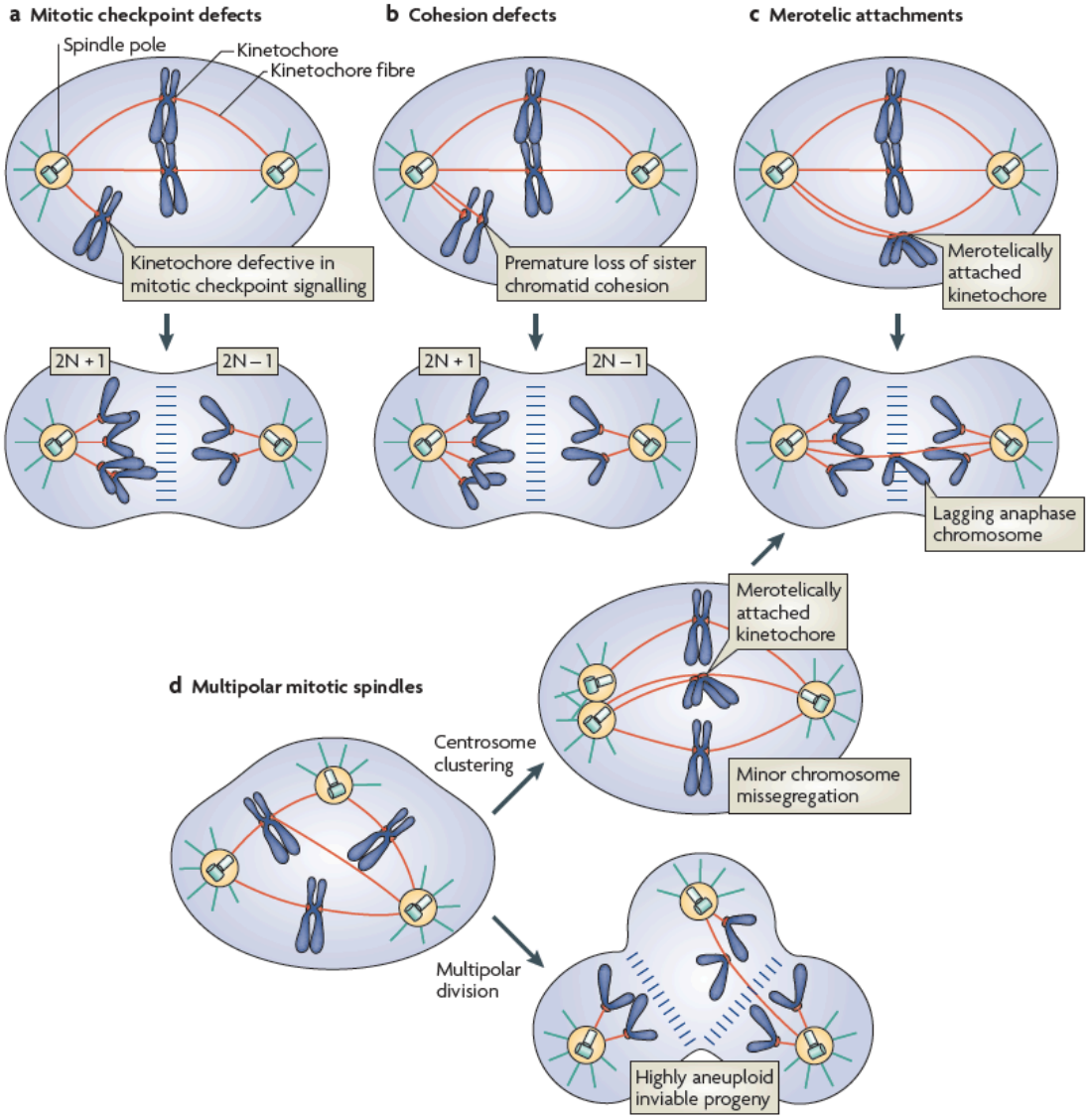

Figure 1.1: Mechanisms of chromosomal missegregation (taken from Holland & Cleveland, 2009).

two centrosomes migrating to opposite poles during mitosis. Additional centrosomes may be introduced through defects in centrosome duplication and result in the generation of multiple poles during cell division (Thompson, Bakhoum, & Compton, 2010). However, aneuploids generated from multipolar divisions are often inviable (Figure 1.1). More commonly, multiple centrosomes will cluster together to form two poles, creating an imbalance in the distribution of spindle microtubules and increasing the frequency

chromosome missegregation caused by merotely (Figure 1.1) (Holland & Cleveland, 2009). Furthermore, aberrations in centrosome number has been found in various human tumors, including malignant breast, prostate, lung, and colon, and have been associated with chromosomal missegregation and resulting aneuploidy (Pihan, 1998).

The Spindle Assembly Checkpoint (SAC) ensures faithful chromosome segregation

Yeast have a robust surveillance mechanism called the spindle assembly checkpoint (SAC) that ensures the equal division of genetic material during mitosis. As described earlier, the main role of the SAC is to halt progression through mitosis by inhibiting the activity of the anaphase promoting complex/cyclosome (APC/C), which binds to and targets downstream cell cycle regulators for degradation by the proteasome (Lara-Gonzalez, 2012). The SAC is activated through its sensing of improper kinetochore-microtubule attachments that generate insufficient tension (Figure 1.2A). The primary components of the SAC – MPS1, Mad1, Mad2, Bub1, Bub3, BubR1 (Mad3 in yeast) – and their interactions are reviewed here.

Assembly of the SAC is initiated by the phosphorylation activity of MPS1, which recruits the BUB1-BUB3 and MAD1-C-MAD2 complex to unattached kinetochores during prophase (Faesen, et al., 2017; Lara-Gonzalez, 2012). The MAD1-C-MAD2 core complex is formed during early mitosis when MAD2 binds MAD1 and transitions from an open (O-MAD2) to a closed conformation (C-MAD2). This complex is then recruited to unattached kinetochores, binds the BUB1-BUB3 complex, and can further recruit cytosolic O-MAD2. The bound O-MAD2 can then bind CDC20, an activator of APC/C, forming the C-MAD2-CDC20 complex and initiating assembly of the mitotic checkpoint complex

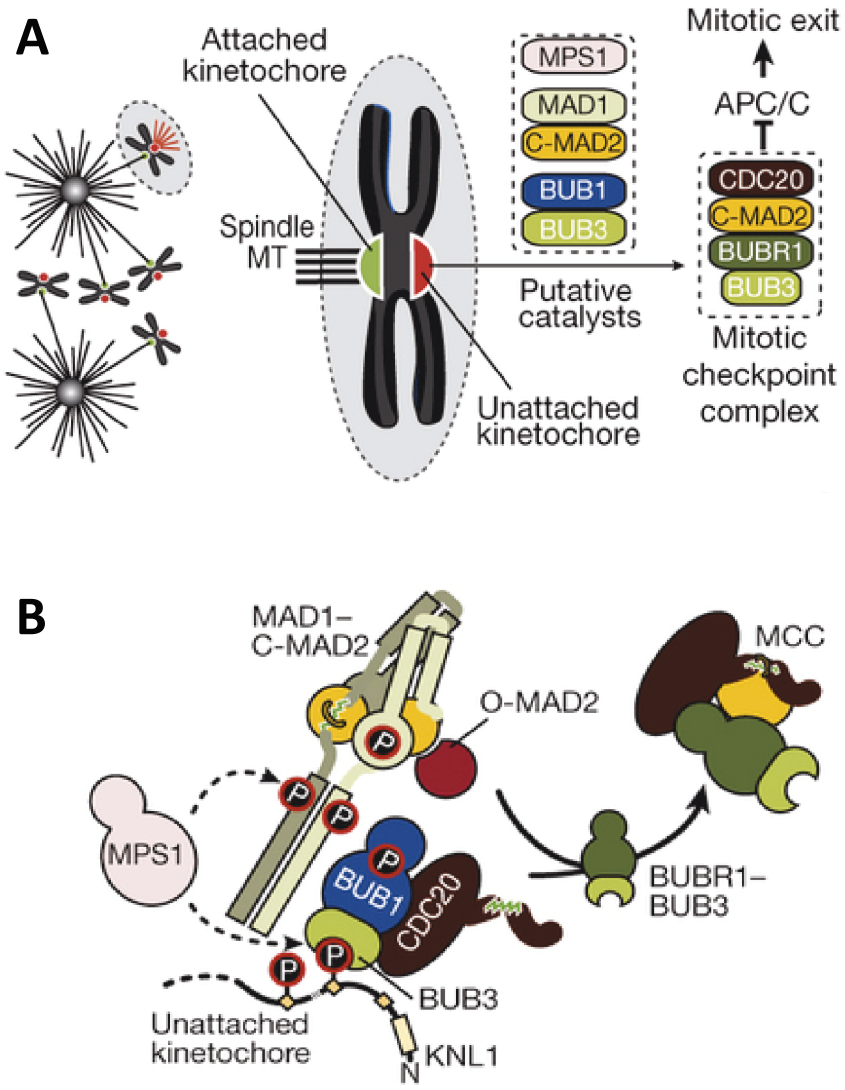

Figure 1.2: The spindle assembly checkpoint. A) The SAC detects unattached kinetochores and delays anaphase by assembling the mitotic checkpoint complex. B) Formation of the mitotic checkpoint complex (taken from Faeson, et al., 2017).

(MCC). The MCC is then fully assembled upon the binding of MAD2-CDC20 and BUBR1(or MAD3)/BUB3, and is the main inhibitor of APC/C (Figure 1.2B). The sequestration of APC/C then halts the cell in metaphase until the proper MT-KT attachments and chromosomal alignments are made. Afterwards, MCC disassembly allows

APC/C to bind to its activator, CDC20, ubiquitinate its downstream targets, and promote mitotic exit (Lara-Gonzalez, 2012).

Measuring chromosomal instability in yeast

Various assays have been developed to measure rates of chromosomal missegregation in yeast. One method that relies on the production of a red pigment was developed several decades ago in *Saccharomyces cerevisiae* and has been used in a genetic screen for mutants with abnormalities in chromosome segregation (Stirling, et al., 2012; Spencer, Gerring, Connelly, & Hieter, 1990). The classical chromosome transmission fidelity (CTF) assay, also known as the colony sectoring assay, makes use of a deficiency in purine biosynthesis caused by a *ade2-101* mutation (Figure 1.3). Incomplete translation of the ade2 enzyme renders the cells unable to complete the synthesis of adenine and, consequently, cells with the *ade2-101* mutation accumulate a visible red pigment. This mutation can be rescued by the presence of a chromosome fragment (CF) containing SUP11 which encodes a tRNA ochre suppressor. Thus, cells that contain the CF are unpigmented whereas cells that lose the chromosome fragment appear red. The loss of the CF can be observed after the fact by visual inspection of individual colonies, and the timing of the loss event can be determined by examining the area of the red sector. For instance, colonies that are half red and half white indicate CF loss during the first cell division after plating, and colonies with one quarter red sectors are indicative of CF loss during the second cell division. While this assay allows for the visual detection of CF loss and calculation of chromosome missegregation rates, tens of thousands of colonies are required in order to obtain an accurate measurement of CF loss rates since chromosomal instability occurs approximately

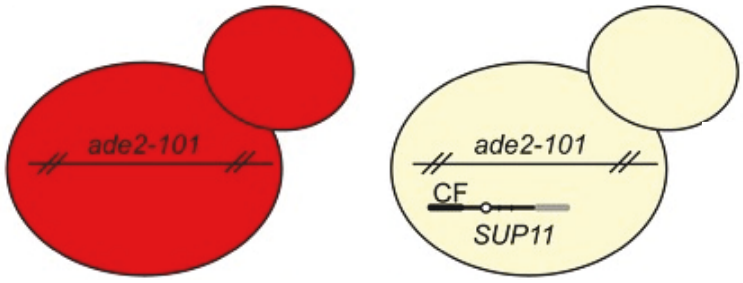

Figure 1.3: The classical chromosome transmission fidelity assay allows for the measurement of chromosome missegregation rates (taken from Stirling, et al., 2012).

once in every 10,000 divisions in this strain (Spencer, Gerring, Connelly, & Hieter, 1990).

Recently, a new method was developed for measuring CIN and similarly utilizes a chromosome fragment, termed "minichromosome" (MC). The quantitative chromosome transmission fidelity (qCTF) assay relies on a reporter/repressor system in which GFP expression is used to detect chromosome loss (Figure 1.4). A reporter consisting of three GFP repeats (3xGFP) is placed adjacent to a mating specific gene, MFA-1, on Chromosome IV. The MC, which is derived form a truncation in the native chromosome III, encodes a strong ✔ repressor that binds to MFA-1 and inhibits the transcription of 3xGFP. Thus, MC loss is indicated by GFP expression and the assay can be used to measure the rate of chromosomal missegregation. By observing the changes in GFP-positive frequency and accounting for the number of doublings, the MC loss rate can be determined. Moreover, flow cytometry can be used to easily detect and distinguish between populations of cells that contain or have lost the MC (Figure 1.4).

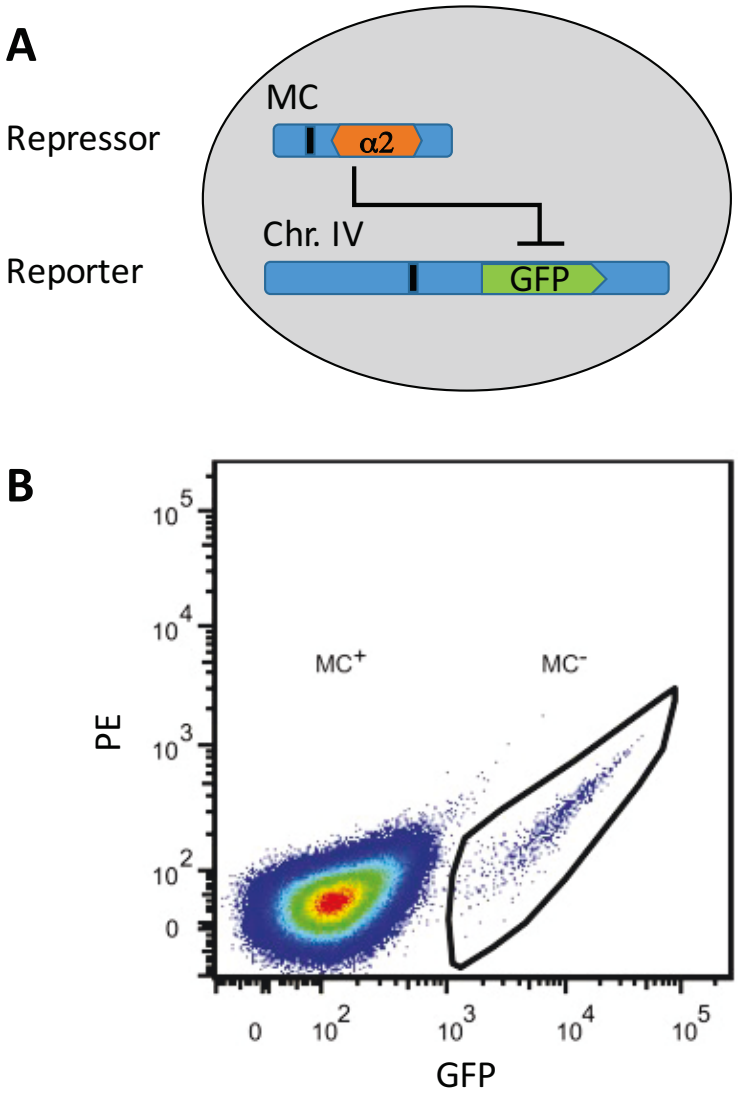

Figure 1.4: The qCTF assay detects minichromosome loss. A) The qCTF assay uses a repressor/reporter module that results in GFP expression when the minichromosome (MC) is lost. B) MC+ and MC- populations are distinguishable through flow cytometry. (Figures are taken from Zhu et al., 2015)

Using a mathematical model, we can quantify the rate of MC loss using only two parameters – the number doublings and the change in GFP-positive frequency. Assuming that events occur on a discrete time scale and equal doubling rates between cells that have the MC and cells that have lost it, the MC loss rate (m) is a function of the initial GFP-positive frequency (R_0), final GFP-positive frequency after n doublings (R_n) and the

number of doublings (n):

$$m = 1 - \left(\frac{1+R_0}{1+R_n}\right)^{\frac{1}{n}} \quad , \quad n = lo\square_2 \frac{N_n^+}{N_0^+}$$

where N_0^+ and N_n^+ denote the initial and final number of cells containing the minichromosome, respectively. (Refer to the Extended Materials and Methods in Zhu, et al., 2015 for full derivation of the equation).

The qCTF assay has several advantages over the classical CTF for a number of reasons. The classical CTF is low throughput and requires the plating of at least 10,000 colonies in order to observe one CF loss event in the wildtype CTF strain. Accurate measurements of CF loss would then require the plating of even more colonies. In contrast, because the qCTF assay uses fluorescence as an indicator of chromosome missegregation, MC loss events can be detected by flow cytometry which can measure the fluorescence of several thousand cells per second. As a result, accurate measurements of chromosomal missegregation can be obtained with significantly reduced labor costs and more samples can be tested simultaneously. Thus, the qCTF assay naturally lends itself for high throughput biology, and is a suitable assay for large genetic or compound screens. Moreover, the qCTF is more sensitive than the classical CTF and is able to detect 2-3 fold changes in chromosome missegregation as demonstrated by a previous study that tested cellular response to treatment with cancer and antifungal drugs (Figure 1.5). The same study found that the qCTF assay is also able to detect approximately 100-fold increases in CIN. As a result, this thesis reports the use of the the qCTF assay for a chemical screen, taking advantage of its high throughput capacity, high sensitivity in detection of small changes in CIN, and large dynamic range.

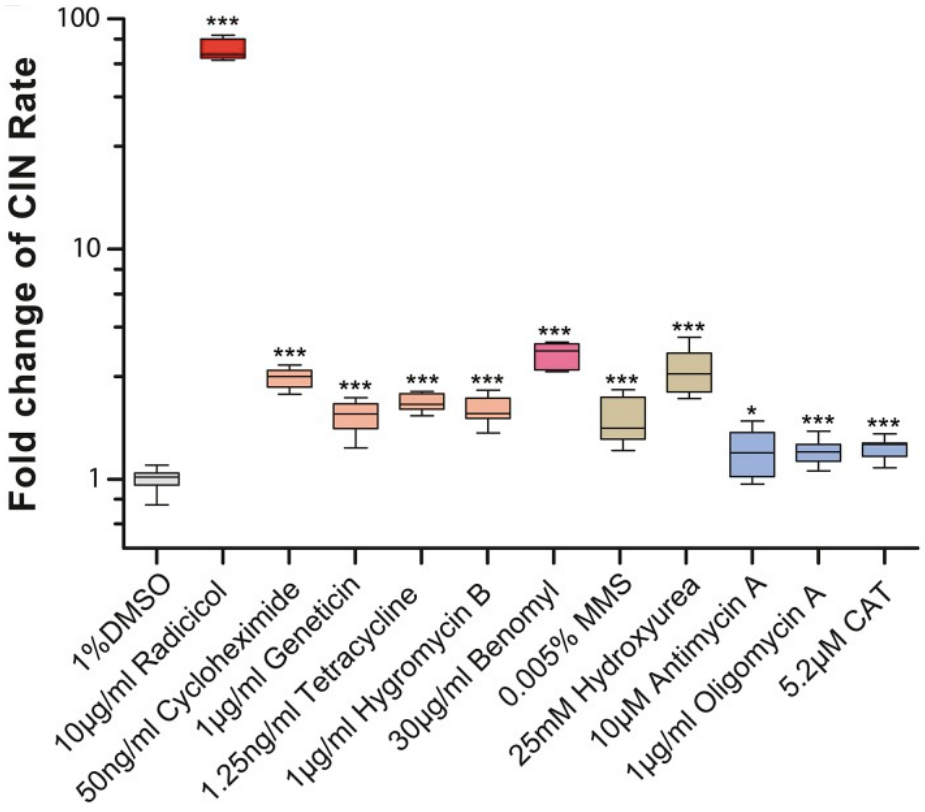

Figure 1.5: The qCTF assay demonstrates sensitive detection of changes in CIN and a large dynamic range (taken from Zhu et al., 2015).

Yeast as a model organism

Saccharomyces cerevisiae is a great model organism for high throughput screens and the study of chromosome segregation for several reasons. Budding yeast have a fast replication time of approximately 100 minutes, can be easily manipulated genetically, and is inexpensive to grow and maintain. The entire genome has been completely sequenced with extensive annotations and can be accessed electronically (Botstein 1999). Moreover, this simple organism is a good model to study chromosome partitioning because several mechanisms and genes involved in chromosome segregation are conserved between between yeast and higher eukaryotes. Additionally, budding yeast can tolerate aneuploidy without severe consequences on cell viability and various established assays exist for

studying chromosome instability in yeast, including a colony sectoring assay, a-like faker assay, and the quantitative chromosome transmission fidelity assay detailed earlier.

Motivation and summary

Provided that there are several routes through which the faithful transmission of chromosomes can be compromised, one can appreciate that chromosome segregation is an intricate and carefully choreographed process. To further elucidate pathways that contribute to chromosome missegregation, the qCTF assay was previously used in a genetic screen to identify mutants with increased or decreased CIN phenotypes. This work extends the study of CIN beyond that of genetic perturbations and investigates the use of the qCTF assay to identify chemical modulators of CIN. We report modifications to the qCTF assay for high throughput compound screens. Moreover, we establish a pipeline that includes false positive exclusion and hit verification procedures, and demonstrate that this optimized qCTF assay can accurately identify potential aneugens in yeast. From our identified hits, we attempt to identify the drug targets of our compound hits in yeast to discover unknown mediators of chromosome segregation.

Chapter 2: Materials & Methods

Chemical transformations in yeast

Yeast transformations were performed as instructed by the micro-scale protocol provided by the Frozen-EZ Yeast Transformation II kit (Zymo Research). An overnight culture grown in SD media was back-diluted to an OD600 of 0.2. The refreshed culture was grown to log phase (OD600 of 0.6) and cells were pelleted in a microcentrifuge at 11000 rpm for 4 minutes. The pellet was then washed with a proportional amount of EZ1 solution and resuspended in EZ2 solution. 5 uL of the deletion cassette (0.2-1 ug DNA) was immediately added to the competent cells and mixed with 100 uL of EZ3 solution. Cells were then incubated at 30°C for 1 hour with occasional vortexing and recovered in 500 uL YPD for 2 hours at 30°C in a rotator. Finally, cells were resuspended in 100 uL autoclaved water, spread onto the appropriate selection plates, and incubated at 30°C for 2-3 days. Strains used in this study were obtained through chemical transformation, sporulation, and/or mating (Table 2.1).

Yeast drop test

The wildtype diploid qCTF strain (RLY8494) and newly generated strains, JZ1270, and JZ1271, were streaked onto YPD plates and incubated at 30 C for 2 days. Single colonies were then inoculated in YPD and grown to saturation at 30 C overnight. Cultures were back-diluted, incubated for 5 hours on a rotator at 30°C and normalized to an OD600 of 0.6. Serial 10-fold dilutions were made from the normalized cultures, and 7 uL of all dilutions were spotted onto drug-treated YPD plates (1% DMSO, 10 ug/mL radicicol, 0.05

ug/ml cycloheximide, 0.4 ug/mL 4-NQO, 10 ug/mL fluconazole, or 5 ug/mL benomyl). The treated plates were incubated at 30 C for two days and scanned.

STRAIN	GENOTYPE
RLY8482	matα, MFA1_3xGFP::HIS5, minichromosome_LEU2
RLY8494	MATa/matα, MFA1_3xGFP::HIS5, minichromosome_LEU2
JZ1270	MATa/matαΔ::NatMX, pdr1Δ::TRP/pdr1Δ::TRP, pdr3Δ::URA3/ pdr3Δ::URA3, erg6Δ::TRP1/erg6Δ::TRP1, minichromosome_LEU2
JZ1271	MATa/matαΔ::NatMX, MAD2/mad2Δ::KanMX6, pdr1Δ::TRP/pdr1Δ::TRP, pdr3Δ::URA3/pdr3Δ::URA3, erg6Δ::TRP1/erg6Δ::TRP1, minichromosome_LEU2
JZ1324	RLY8494 STE11 del with KanMX6
JZ1325	RLY8492 BMH1 del with KanMX6
JZ1326	RLY8494 HOG1 del with KanMX6
JZ1327	RLY8494 PBS2 del with KanMX6
JZ1330	RLY8494 BMH1 del with KanMX6
JZ1332	RLY8492 YLR345W del with KanMX6

Table 2.1: Strains used in this study. For more details on strains RLY8492 and RLY8494 refer to Zhu, et al., 2015.

High throughput kinase inhibitor screen procedure

Kinase inhibitors were resuspended in DMSO to a final concentration of 1 mM and were aliquoted into five 96-well PCR plates such that the last column of all 96-well PCR plates contained only DMSO controls in order to control for edge effects. JZ1271 was inoculated into SD –leucine media to select for cells containing the minichromosome and allowed to grow at 30° C for 24 hours on a rotator. The initial GFP-positive frequency of the overnight culture was measured the next day using an Attune Nxt Flow Cytometer (Invitrogen). Overnight cultures were then back-diluted to an OD600 of 0.01 in SD media and

transferred into 96-deep well plates using a multichannel pipette. An EpMotion 5075 automated liquid handler (Eppendorf) was then used to treated individual wells with kinase inhibitors for a final inhibitor concentration of 10 uM, 1% DMSO, or left untreated. The cultures were allowed to grow for 24 hours shaking at 200 rpm and 30°C. The final OD600 was measured with a plate reader. Samples were then pelleted in a 96-well microtiter plate, fixed in an equal volume of 4% PFA for 15 minutes, washed twice with PBS supplemented with 1% YEP, and resuspended in an equal volume of PBS. During the fixation, samples were pelleted by centrifugation at 3000 rpm for 3 minutes and resuspended by shaking at 1000 rpm for 3 minutes. Aliquots of fixed samples were diluted in PBS and samples from all four plates were compiled into a single 384 deep well plate using the automated liquid handler. The final GFP-frequency was then measured using an Attune Nxt Autosampler (Invitrogen), and the minichromosome loss rate was calculated for all samples. Four biological replicates were tested for each kinase inhibitor.

Flow cytometry data collection

0.3 million events were recorded for each sample in 1.5 mL Eppendorf tubes or 96-well microtiter plates. Cells were gated on FSC-H vs. SSC-H channels, single cells were gated on SSC-H vs SSC-A channels, and GFP-positive populations were gated on BLH1-H vs YLH1-H channels.

Calculating minichromosome loss rate

The initial GFP-positive frequency, final GFP-positive frequency, and number of generations (calculated from the initial OD and final OD) were used to calculate loss rate.

Loss rate *m* and generations *n* are given as:

$$m = 1 - \left(\frac{1+R_0}{1+R_n}\right)^{\frac{1}{n}} \quad , \quad n = log_2\left(\frac{N_n^+}{N_0^+}\right)$$

(refer to the "Measuring chromosomal instability in yeast" section in Chapter 1 for more details).

High throughput screen data analysis

To determine and remove outliers for each kinase inhibitor, leave-one-out cross validation (LOOCV) was used to evaluate the ratio of the final GFP-positive frequency (R_n) to the initial GFP-positive frequency (R_0) across all four biological replicates for each inhibitor. Briefly, $\frac{R_n}{R_0}$ was calculated for all four biological replicates and a t-statistic was calculated for three randomly chosen biological replicates. The remaining replicate was excluded as an outlier if its $\frac{R_n}{R_0}$ ratio was not within the 95% confidence interval. The same method was used to exclude outliers in the number of generations for biological replicates. Replicates with negative generations were excluded since these cells either exhibit reduced growth or were killed under drug treatment. CIN rate was calculated for the remaining replicates and normalized to DMSO controls across all plates to determine the CIN fold change. The average CIN fold change of each inhibitor was calculated and inhibitors were ranked from lowest to highest CIN fold change.

Cell sorting and auxotrophic growth assay

JZ1271 (the qCTF strain used for the kinase inhibitor screen) was inoculated into SD -leucine media and cultured on a rotator at 30°C for 24 hours. JZ1271 was then back-diluted

1:500 and treated with 1% DMSO (solvent control) or S1070 to a final concentration of 10 uM and grown for 24 hours at 30°C. Gates were drawn for each sample based on their GFP profiles, and 300 cells from each gated population were sorted using a DakoCytomation MoFlo (Johns Hopkins University Flow Cytometry and Cell Sorting Core Facility) into liquid YPD media and plated onto individual YPD plates. After incubation in 30°C for 2 days, the number of colony forming units per plate was counted using Fiji. Each YPD plate was then replica plated onto SD –leucine plates and grown in 30°C for 2 days. The number of colonies that grew on SD –leucine plates were counted to determine the percentage of colonies that retained the minichromosome.

PI staining

Staining with propidium iodide was performed by the JHU Flow Cytometry and Cell Sorting Core Facility immediately after cell sorting using standard protocols.

Colony sectoring assay

RLY4030 was streaked onto SD –uracil plates and incubated at 30 C for 2-3 days. A single colony was then inoculated into SD –uracil media and grown in 30 C overnight on a rotator. Cells were then refreshed in SD media the next day and allowed to double for 5 hours. Cells were back-diluted in 5 mL of SD media treated with the appropriate concentration of drugs for 5 hours (1 % DMSO, 10 ug/mL radicicol, 100 uM RAF265, 100 uM dabrafenib, 100 uM MK-5108, or 100 uM PFK15). Cultures were then washed twice with water, resuspended in 1.5 mL autoclaved water and sonicated. The optical densities of the resuspended cultures were then measured, cultures were diluted to 2,400 cells per mL in

water, and plated onto 150 mm-diameter SC low adenine plates at 600 cells per plate. Plates were incubated at room temperature for 3 days, and stored at 4 C to allow sufficient time for pigment accumulation. Plates were then scanned and the total number of colonies per plate was quantified by Fiji. Colonies on the edges of the plate were excluded. Since cells deficient in adenine biosynthesis were observed to grow marginally slower, half-sectors were defined as colonies in which the red sector comprised more than 33% of the colony area (as quantified by Fiji). Chi-square analyses were performed in GraphPad to quantify differences in CIN between treated and DMSO control samples.

Chapter 3: Results and Discussion

Adapting the qCTF assay for a high throughput screen

In order to identify inhibitors that increase chromosomal instability from a commercially-available library of kinase inhibitors, the existing qCTF assay was modified to increase high throughput screening efficiency. The qCTF assay was previously used to test a small selection of compounds that were either known or speculated to elevate CIN (Zhu, et al., 2015). Drug concentrations required to produce detectable fold changes in CIN were in the high micromolar range, occasionally requiring concentrations as high as 25 mM in order to detect 6-fold changes. The need for high drug concentrations highlights a major limitation of the qCTF assay for cost-effective high throughput compound screening. Notably, this limitation is not unique to the qCTF assay alone – various compound screens in yeast have encountered similar complications. In a small selective screen of 31 anticancer drugs conducted in wildtype yeast, the IC50 was observed to be greater than 100 uM for the majority of drugs and greater than 1 mM for approximately one quarter of the compounds tested (Simon, et al., 2000). Extensive studies have investigated various membrane transport proteins expressed on the plasma membrane of wildtype yeast that aid in pumping small molecules, including drugs and hormones, out of the cell (Ernst, Klemm, Schmitt, & Kuchler, 2005; Moye-Rowley, 2003; Nourani, Wesolowski-Louvel, Delaveau, Jacq, & Delahodde, 1997; Balzi & Goffeau, 1995). Efficient and cost-effective compound screens in yeast exploit the increased drug sensitivity conferred by the deletion of genes regulating drug efflux pumps and membrane permeability (Balzi & Goffeau, 1995; Perkins, et al., 2001; Dunstan, et al., 2002).

To increase the drug sensitivity of the qCTF strain, three well-characterized

genes—ERG6, PDR1, and PDR3—were deleted and replaced with auxotrophic selection markers, TRYP1 (used redundantly) and URA3 (refer to Table 2.1). ERG6 is a methyltransferase involved in the biosynthesis of ergosterol, a component of the plasma membrane that contributes to its fluidity and permeability (McCammon, Hartmann, Bottema, & Parks, 1984; Emter, Heese-Peck, & Kralli, 2002; Sharma, 2006). The deletion of ERG6 has been shown to increase the passive diffusion of drugs across the plasma membrane (Emter, Heese-Peck, & Kralli, 2002). In contrast, pdr1 and pdr3 transcriptionally regulate the expression of multi-drug resistance efflux pumps on the plasma membrane, thereby regulating the concentration of small molecules in the cell (Balzi & Goffeau, 1995). Deleting these three genes simultaneously increases membrane permeability while decreasing small molecule efflux, allowing for a higher local concentration of drugs inside the cell at low dosages of drug treatment. Moreover, the combinatorial deletion of these three genes is common in compound screens—as an example, the National Cancer Institute used a yeast strain containing these same gene deletions to identify small molecules that could selectively kill mutants deficient in double-strand break repair mechanisms (Dunstan, et al., 2002).

For the purpose of our study, we generated a diploid qCTF strain with homozygous deletions in ERG6, PDR1, and PDR3 (JZ1270). To test for drug sensitivity, a drop test was performed whereby serial dilutions of each strain were spotted onto YPD plates treated with individual drugs and the strains were allowed to grow for 2-3 days (Figure 3.1). The homozygous deletion mutant showed reduced growth on plates treated with cycloheximide, radicicol, 4-nitroquinoline 1-oxide, benomyl and DMSO (solvent control), indicating increased drug sensitivity to most drug treatments relative to the wildtype qCTF

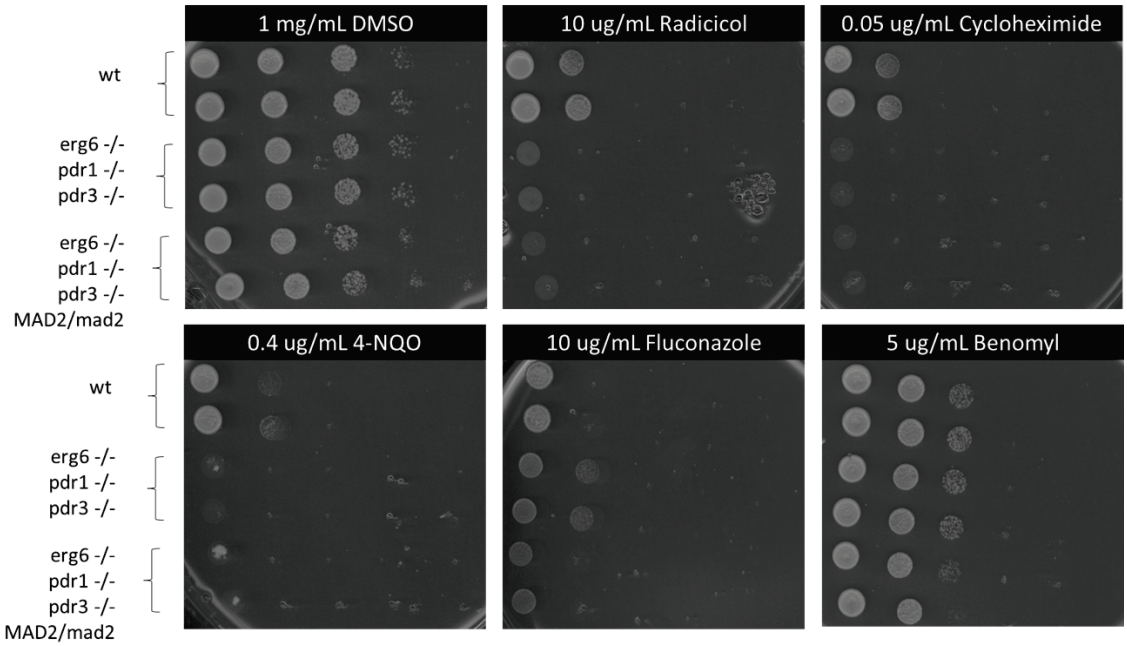

Figure 3.1: Homozygous deletion of genes regulating membrane permeability and efflux pumps increases drug sensitivity. Drop tests were performed for two biological replicates of three different strains grown on YPD plates treated with 1% DMSO (solvent control), 10 ug/mL radicicol, 0.05 ug/ml cycloheximide, 0.4 ug/mL 4-NQO, 10 ug/mL fluconazole, or 5 ug/mL benomyl. The top two rows of each plate represent the wildtype qCTF strain with intact membrane and drug pumps, followed by two biological replicates of the qCTF strain with homozygous drug pump deletions, and two biological replicates of a drug sensitive qCTF strain containing a heterozygous deletion of MAD2. Columns represent serial 10-fold dilutions of each strain.

strain. Interestingly, these homozygous drug pump deletions increase resistance to treatment with an FDA-approved antifungal agent, fluconazole (Vandeputte P. F., 2011). This is may be explained by reported observations that ERG6 mutants demonstrate increased resistance to fluconazole (Mukhopadhyay K. K., 2002).

In addition to exhibiting increased drug resistance, yeast also have a robust surveillance mechanism to ensure the even distribution of genetic material during mitosis called the SAC (reviewed in Chapter 1). Failure to correct errors that arise during chromosome segregation often results in cell death. Thus, in order to observe increases in chromosomal missegregation events without inducing cell death, it is necessary to weaken

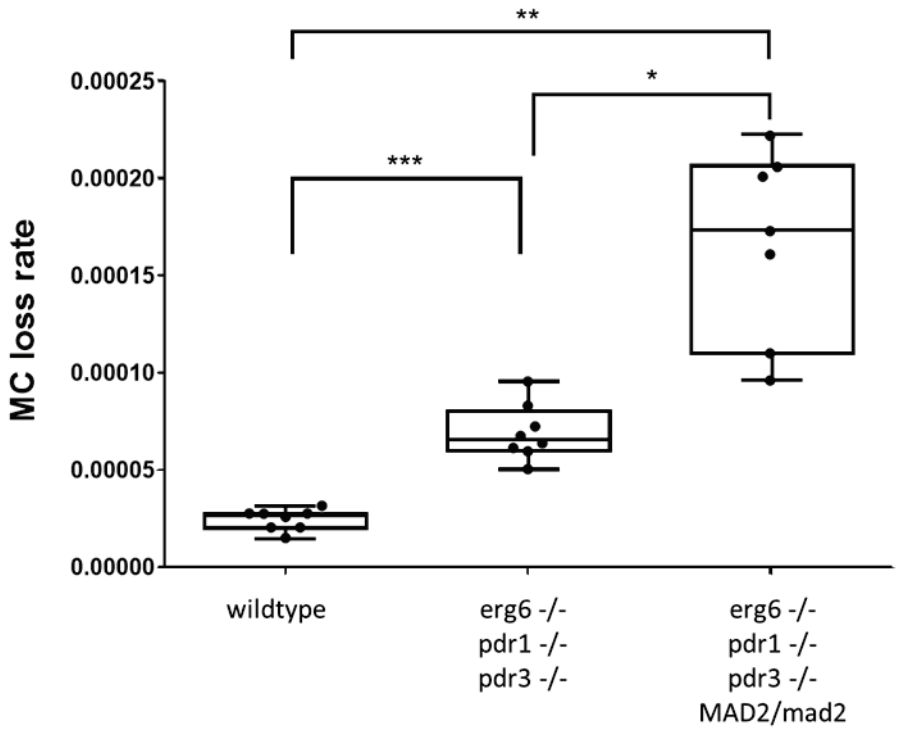

Figure 3.2: Heterozygous deletion of MAD2 weakens the mitotic checkpoint and increases basal CIN rate in yeast ($p = 0.0014$). Increasing drug sensitivity also imparts a 2.5-fold increase in the CIN rate ($p < 0.0001$). All mutations are synergistic and increase CIN by roughly 6-fold ($p = 0.0002$). n = 8 biological replicates per strain, treated with 1% DMSO. (* $p < 0.01$, ** $p < 0.001$, *** $p < 0.0001$). Observed median CIN rates were 2.67E-5 per cell division for the wildtype qCTF strain, 6.57E-5 per cell division for the drug sensitive strain, and 1.73E-4 per cell division for the drug sensitive strain with a heterozygous MAD2 deletion.

the robust mitotic checkpoint, thereby allowing the cell to tolerate errors that arise during cell division. Surprisingly, interfering with the expression of drug pumps and membrane permeability alone elevate CIN by roughly 2.5-fold (Figure 3.2).

To further increase CIN, we deleted a crucial component of the spindle assembly checkpoint, MAD2 (reviewed in Chapter 1). A strain (JZ1271) with a heterozygous deletion of MAD2 and homozygous deletions of ERG6, PDR1, and PDR3 was generated and its basal CIN was determined. As predicted, the heterozygous MAD2 deletion allows

the cell to tolerate chromosomal missegregation events and demonstrates a synergistic effect with the homozygous drug pump deletions, providing an additional 2.5-fold increase in CIN (Figure 3.2). Consequently, the resulting strain elevated CIN by a total of 6-fold, with a median CIN rate of 1.73E-4 per cell division, and was chosen for our kinase inhibitor screen.

Identifying hits from a primary screen

The adapted qCTF assay was used to identify aneugens from a commercially-available library of 418 kinase inhibitors purchased from Selleckchem (refer to Chapter 2 for screen design). From our initial screen, we observed 20 kinase inhibitors that increase CIN by more than 5-fold, 16 inhibitors that increase CIN by more than 10-fold, and 2 inhibitors that increase CIN by more than 100-fold (Figure 3.3). Additionally, 3 inhibitors decreased CIN by 5-fold, resulting in CIN rates lower than 1.5×10^{-5}. However, because these low CIN measurements approached the detection limit of the modified qCTF assay, we could not demonstrate with statistical significance that these inhibitors decreased CIN. As a result, we focus only on kinase inhibitors that elevate CIN for the remainder of this study.

Interestingly, tyrosine kinase inhibitors were amongst the top 10 kinase inhibitors that elevate CIN, two of which comprised the top two hits and target the mammalian kinase, c-met, for which there is no yeast homolog (Figure 3.4). In addition to tyrosine kinases (which make up approximately 25% of the kinase inhibitor library) other pathways that comprised the majority of our top hits include MAPK (11%) and mTOR (23%). Moreover, the kinase inhibitor hits that increase CIN by more than 5-fold are distributed across a wide array of pathways (Figure 3.4).

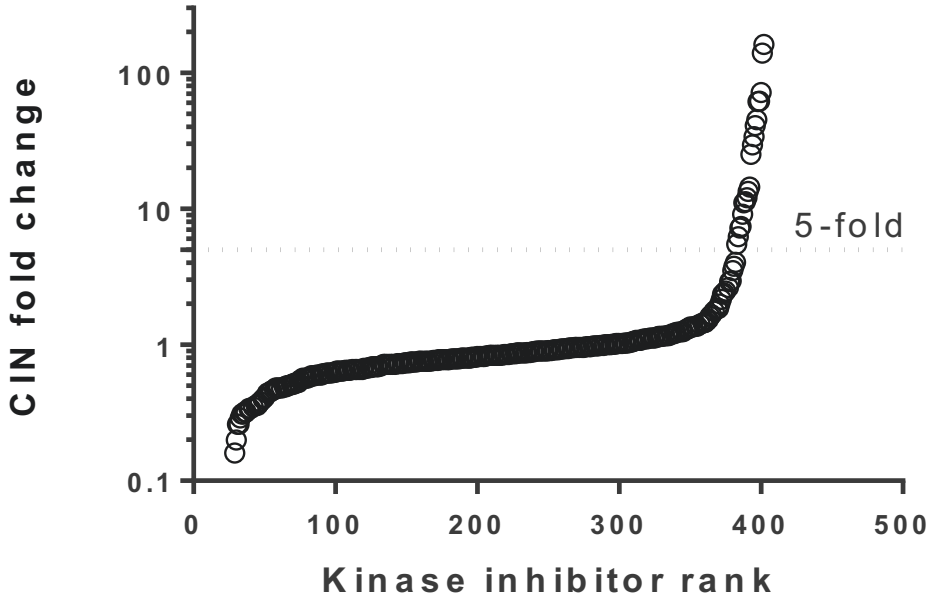

Figure 3.3: 20 kinase inhibitors increase CIN rate by more than 5-fold and up to about 200 fold.

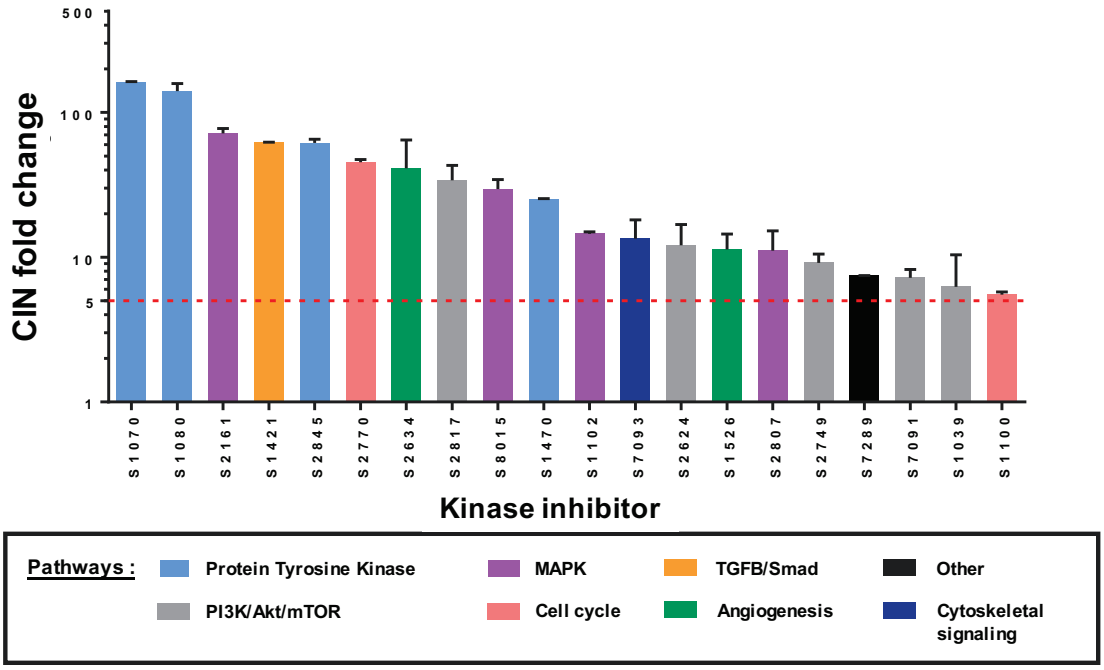

Figure 3.4: The distribution of pathways targeted by the top 20 kinase inhibitors reveal a diverse set of pathways that induce significant CIN fold changes, the common pathways being protein tyrosine kinase, MAPK and mTOR.

Identifying and excluding false positive hits

Although 20 kinase inhibitors increased CIN by more than 5-fold, abnormal GFP profiles were observed in several of these samples. Unidentified populations that span the gap between MC+ and MC- populations were observed and confounded the quantification of GFP-positive frequencies required for CIN calculations (Figure 3.5). Of the top 10 kinase inhibitors that increase CIN, 5 inhibitors gave rise to abnormal GFP profiles including our top two putative hits. Interestingly, all 5 inhibitors were yellow in color and 4 of the 5 inhibitors were identified as tyrosine kinase inhibitors (Table 3.1). However, this was not a common GFP signature of all tyrosine kinase inhibitors since the tyrosine kinase inhibitor providing the next highest CIN fold increase (S1179) did not produce an abnormal GFP profile (Figure 3.5).

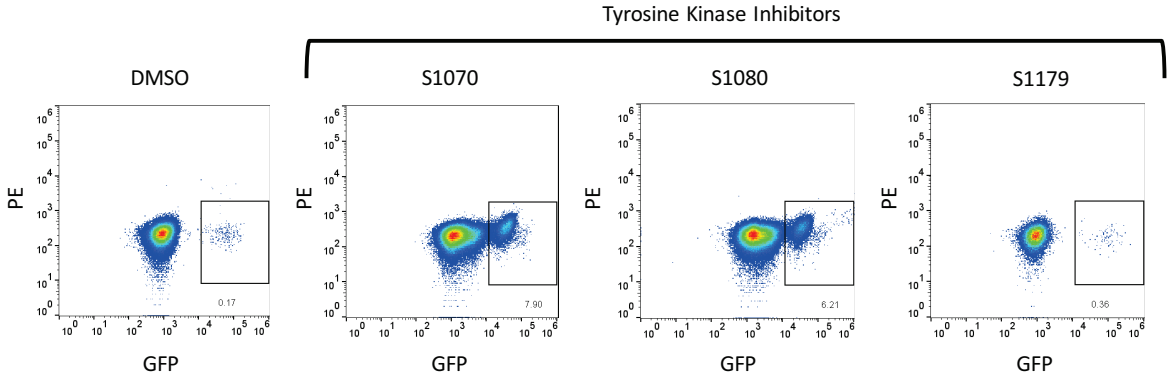

Figure 3.5: Abnormal GFP profiles were observed in some treated samples. GFP profiles showing distinct GFP-positive (gated in black) and GFP-negative populations in samples treated with 1% DMSO (solvent control) or protein tyrosine kinase inhibitors (S1070, S1080, and S1179) that were yellow in color. Unexpected populations were observed in samples treated with tyrosine kinase inhibitors that comprised our top two putative hits, S1070 and S1080. In contrast, these abnormal profiles were absent in both the DMSO control and sample treated with S1179 – the next highest tyrosine kinase inhibitor producing the 28th highest increase in CIN.

To investigate the source of these unidentified populations, we sorted cells from each population and tested the cells for the presence of an auxotrophic marker, LEU2, which was only present on the minichromosome. The strain used for the kinase inhibitor

Inhibitor	Product Name	CIN fold change	Color	Pathway	Targets
S1070	PHA-665752	162	Yellow	Tyrosine kinase	c-Met
S1080	SU11274	140	Yellow	Tyrosine kinase	c-Met
S2161	RAF265	71.7		MAPK	VEGFR, Raf
S1421	Staurosporine	62	Yellow	TGFB/Smad	PKC
S2845	Semaxanib	61.5	Yellow	Tyrosine kinase	VEGFR
S2770	MK-5108	45.2		Cell Cycle	Aurora Kinase
S2634	Rebastinib	41		Angiogenesis	Bcr-Abl
S2817	Torin 2	33.9		PI3K/Akt/mTOR	mTOR, ATM/ATR
S8015	CEP-32496	29.5		MAPK	CSF-1R, Raf
S1470	Orantinib	25.2	Yellow	Tyrosine kinase	PDGFR, FGFR, VEGFR

Table 3.1: Top 10 putative kinase inhibitors hits that elevate CIN, their pathways, targets and drug color. Half of the putative top hits are yellow in color, and 4 of the colored inhibitors target the tyrosine kinase pathway**.**

screen (JZ1271) was treated with either solvent control (1% DMSO) or our putative top hit (S1070). Cells were then sorted into populations containing 300 cells per population: MC+, MC-, and any unidentified populations. Each population was grown on individual YPD plates and the resulting colonies were then counted and replica plated onto SD –leucine plates to quantify the percentage of cells that retained the mini chromosome. Only 6 of the 300 cells from the unidentified populations grew into colonies, suggesting that the population consisted primarily of dead cells and indicating an initial overestimation of the GFP-positive population (Figure 3.6). A small decrease was observed in the MC- populations of both DMSO and S1070 treated samples, possibly as a result of cytotoxicity caused by high GFP expression. Moreover, a small percentage of the MC- population in all treated samples contained cells that have retained the minichromosome (about 5% on average). These relative proportions of these MC-positive cells is small and has minimal

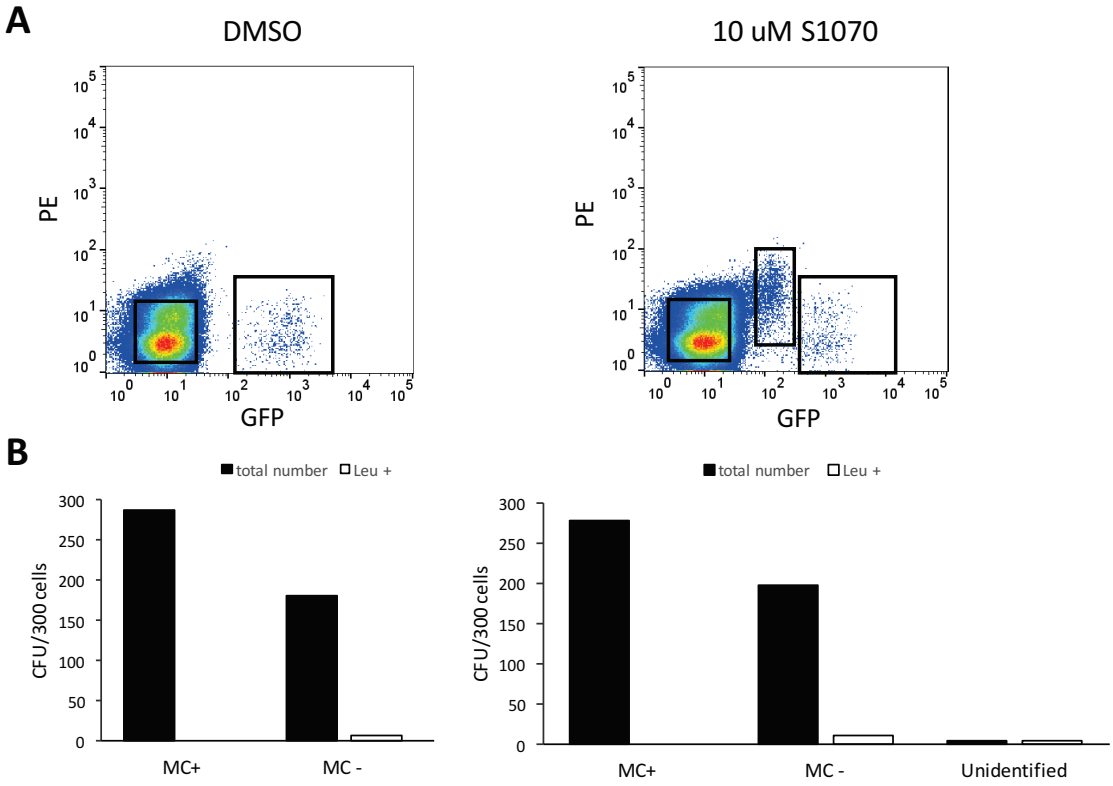

Figure 3.6: Unidentified populations are comprised of dead cells. A) The GFP profiles of samples treated with 1% DMSO or 10 uM S1070 (the putative top hit) are depicted. Cells from GFP-negative, GFP-positive, and/or mystery populations were sorted (boxes indicate the populations that were collected) and plated onto YPD. B) Quantification of the colony forming units that arose from the 300 cells sorted show that the unidentified population is comprised of only 6 cells. Black bars indicate the total number of colony forming units, and white bars indicate the number of colonies that grew on SD – leucine plates.

effects on the calculated CIN rate. To further reduce this percentage, we can increase the stringency of our gating to further increase the accuracy of our GFP-positive frequency measurements.

The presence of dead populations was further validated by staining treated samples with an excitable viability dye, propidium iodide, which penetrates the damaged membranes of dead cells and intercalates into double stranded DNA (R&D Systems, 2017). Flow cytometry was used to detect cells that accumulated the viability dye and the percentage of dead cells was quantified (Figure 3.7). PI staining identified small

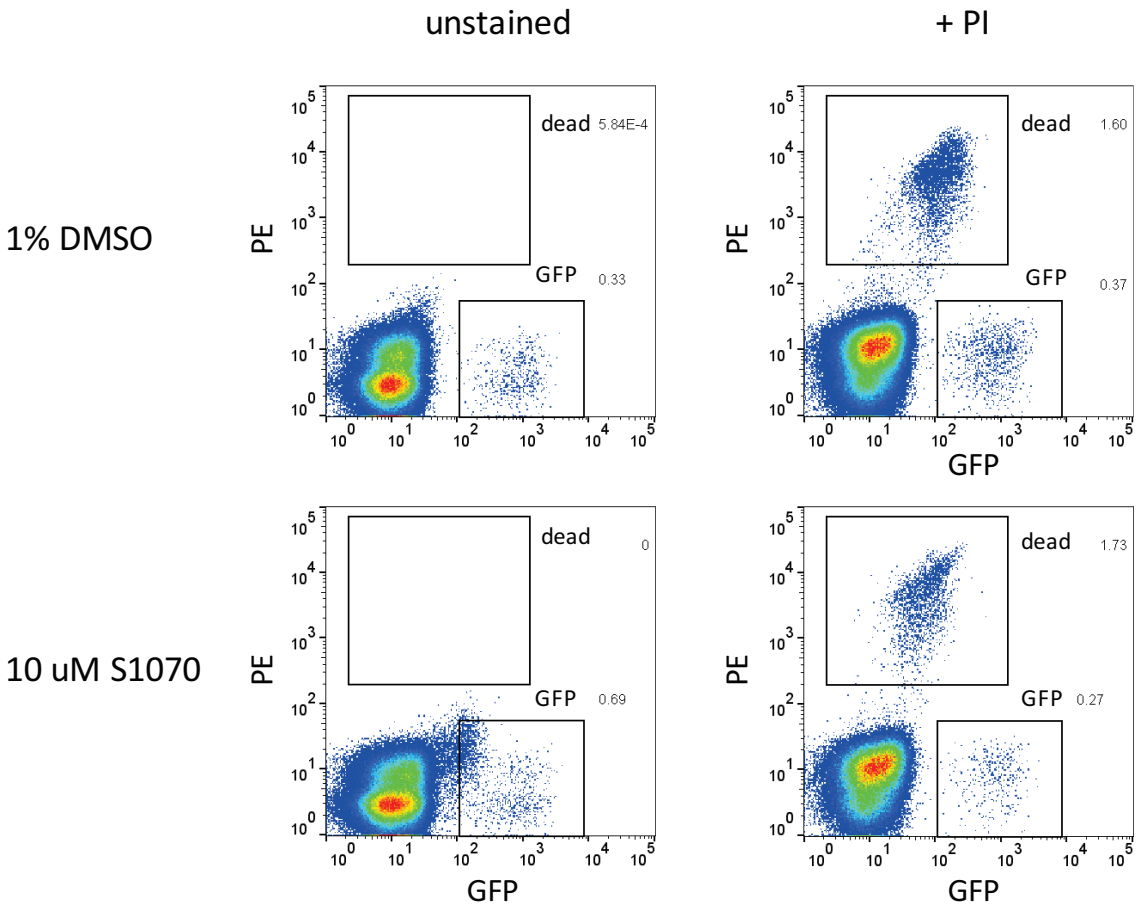

Figure 3.7: PI staining reveals that the unidentified population is comprised of dead cells stained with drug. The top row depicts the control sample treated with 1% DMSO and the bottom row depicts the sample treated with kinase inhibitor, S1070. The GFP profiles of each sample are shown before (left column) and after (right column) PI staining.

percentages of dead cells in both the DMSO control and sample treated with 10 uM S1070. Notably, the absence of the unidentified population after PI staining suggests that the unidentified population is comprised of dead cells stained with the inhibitor. Taken together, cell sorting and viability staining suggest that the abnormal GFP profiles observed arose from dead cell populations that were stained by the colored kinase inhibitors and detected by the PE channel used. Staining of dead populations resulted in the overestimation of the population's GFP-positive frequency and CIN. Subsequently, all

kinase inhibitors with abnormal GFP-positive profiles (S1070, S1080, S1421, S2845 and S1470) were excluded from the top hits (Table 3.1). Additional experiments conducted after the completion of the kinase inhibitor screen revealed that these dead populations of stained cells could be observed under the BLH2 channel. These results demonstrate the disadvantages of using fluorescence-based assays for compound screens and speak to the importance of obtaining measurements using multiple channels during the screening process to facilitate the identification of false positive hits afterwards. Moreover, screen design that allows for non-colorimetric validation of putative hits (i.e., phenotypic validation) provides additional routes of effective false positive hit identification.

An additional parameter used to rule out false positives was the number of doublings undergone in 24 hours. Since opportunities for chromosomal missegregation only arise during mitosis and occur at a rate of approximately 1×10^{-4}, a sufficient number of cell divisions is required for accurate CIN measurements. More frequent cell divisions facilitate the accurate measurement of GFP-positive frequencies. Consequently, 24 of the remaining kinase inhibitors, which were observed to slow cell proliferation to fewer than 4 generations in 24 hours, were removed from further analysis (Figure 3.8). Although these inhibitors were excluded from our screen for compounds that increase chromosomal instability, they may be useful as novel fungicides. Further testing in mammalian cells is required to investigate inhibitor cytotoxicity, selectivity, and potential for drug repurposing.

After removing the false positive hits and drugs that inhibit cell growth and proliferation, we identified four kinase inhibitors hits that increase CIN by more than 5-fold (Figure 3.9). Our top two hits are both ATP-competitive inhibitors affecting the

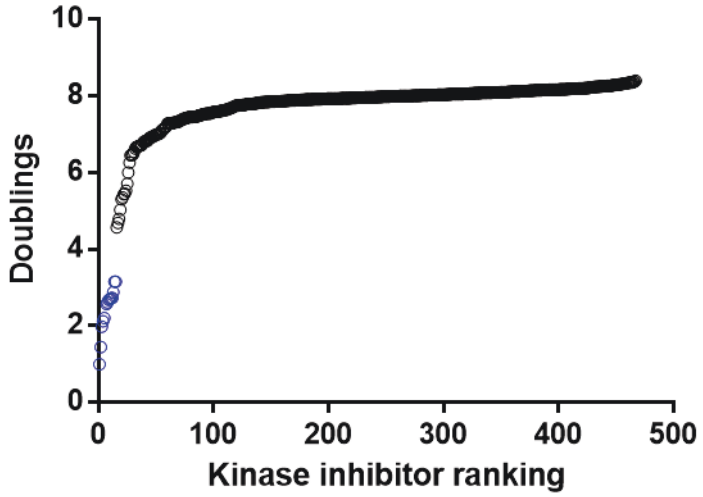

Figure 3.8: 24 kinase inhibitors reduce cell proliferation to fewer than 4 generations in 24 hours. These inhibitors that slow cell growth and proliferation and were excluded from further analysis.

MAPK pathway, which regulates cell proliferation, differentiation and apoptosis (Jin, Jiang, Rosen, Nelkin, & Ball, 2011; Holderfield, Nagel, & Stuart, 2014; Zhang & Liu, 2002; Morrison, 2012). RAF265 produced the highest CIN fold change and has been shown to interfere with cell proliferation and tumor angiogenesis by inhibiting c-raf, wildtype b-raf, and mutant b-raf (V600E) and preventing VEGFR2 phosphorylation with an IC50 in the nanomolar range (Table 3.2) (Williams, et al., 2015; Selleckchem, 2017). In the past decade, RAF265 has been tested in Phase II clinical trial by Novartis for the treatment of metastatic melanoma initiated in 2006 and in combination with other chemotherapy agents in 2011 (Pharmaceuticals, Novartis, 2016; Array BioPharma, 2016). Acting in the same pathway is dabrafenib, our second hit and selective FDA-approved inhibitor (IC50 = 0.65 nM) for the treatment of melanomas harboring the BRAF V600E mutation (GlaxoSmithKline, 2014). In a phase III clinical trial, dabrafenib significantly increased

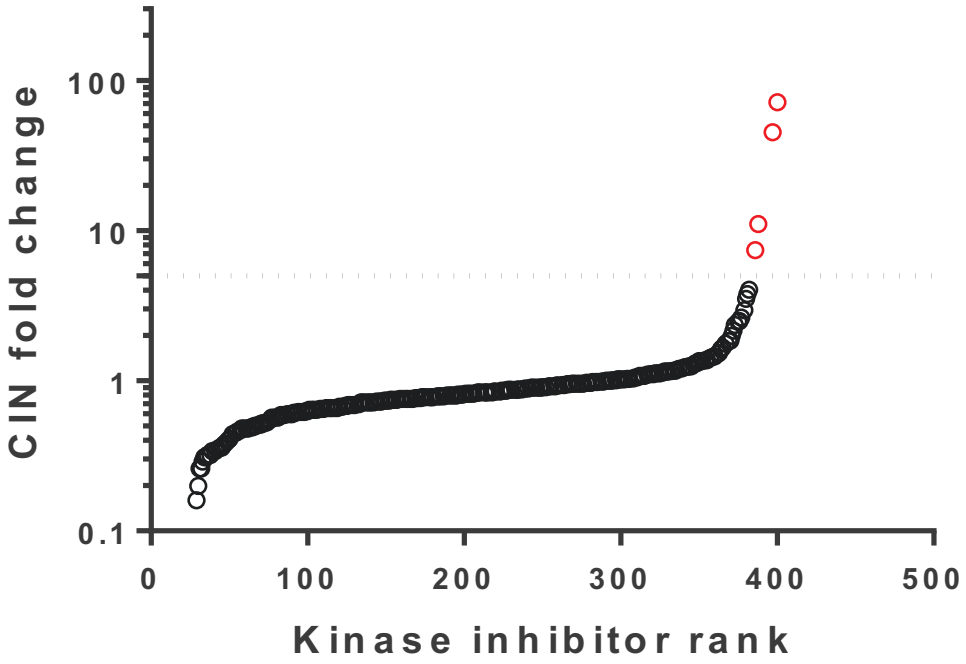

Figure 3.9: The remaining kinase inhibitor hits that increase CIN by more than 5-fold after excluding false positives and drugs that inhibit cell growth/proliferation.

Inhibitor	Target	Pathway
RAF265	C-Raf/B-Raf/B-Raf V600E	Raf signaling pathway
Dabrafenib	B-Raf V600E	Raf signaling pathway
MK-5108	Aurora A	Aurora Kinase signaling pathway
PFK15	6-phosphofructo-2-kinase (PFKFB3)	AMPK signaling pathway

Table 3.2: The four kinase inhibitor hits, their mammalian targets and pathways.

progression-free survival to a median of 5 months in a cohort of 187 patients as compared with dacarbazine, which was the standard chemotherapy treatment for metastatic melanoma (Hauschild, et al., 2012).

Our third hit is an Aurora A-specific kinase (IC50 = 0.064 nM) and ATP-competitive inhibitor that interferes with a key regulator of mitosis and arrests the cell in G2/M phase (Shimomura, et al., 2010). Perturbations in the expression and function of aurora A have been demonstrated to cause chromosomal instability. Overexpression of Aurora A is observed in numerous human cancers, including breast, ovarian, colorectal and skin, and has been implicated in conferring drug resistance to Taxol, a commonly administered chemotherapy agent (Nikonova, Astsaturov, Serebriiskii, Dunbrack, & Golemis, 2013; Anand, Penrhyn-Lowe, & Venkitaraman, 2003). Additionally, silencing Aurora A causes centrosome missegregation, abnormal spindle assembly, and chromosomal misalignment (Marumoto, et al., 2003). Given that reduction in Aurora A expression has been implicated in chromosomal instability, this inhibitor is a positive hit that provides further validation in support of the hits identified by our screen. Notably, this Aurora A kinase inhibitor demonstrates anti-tumorigenic activity, showing promising results in a recently completed phase I study for use as monotherapy and combination therapy with docetaxel to treat advanced solid tumors (Shimomura, et al., 2010; Amin, et al., 2016).

Our final hit is a 6-phosphofructo-2 kinase (PFKFB3) inhibitor, which has a high IC50 of 207 nM (Clem, et al., 2013). PFKFB3 is overexpressed in aggressive breast, ovarian, and thyroid cancers and has been shown to promote cell cycle progression (Yalcin, et al., 2014; Atsumi, et al., 2002). Studies have demonstrated that inhibition of PFKFB3 in

HeLa cells reduces glycolysis and glucose uptake, decreases cell proliferation, and induces apoptosis (Yalcin, et al., 2014). Moreover, PFKFB3's role in increasing cell proliferation is not limited to its production of 2,6-biphosphate, an activator of glycolysis, and has been implicated in modulating p27 expression in the nucleus through proteasome degradation (Yalcin, et al., 2014). Consequently, many studies have explored the suppression of PFKFB3 as a potential cancer therapeutic leading to a phase I clinical trail initiated in 2014 for the use of a newly optimized PFKFB3 inhibitor, PFK-158, to treat advanced solid malignancies (Clem, et al., 2013; Redman, Pohlmann, Kurman, Tapolsky, & Chesney, 2015). Although PFKFB3 has been linked to cancer through increased glucose metabolism and suppression of apoptosis, how it induces chromosomal instability remains unknown.

Validation of top hits using a classical qCTF assay

Each of the hits was verified using a classical chromosome transmission fidelity assay (described in Chapter 1). A haploid CTF strain harboring an *ade2-101* mutation and a chromosome fragment containing SUP11 (as previously used by Spencer et. al., 1999 and Zhu et. al., 2015) was used to validate our top hits. This strain was treated with either solvent control (1% DMSO) or inhibitors, and the percentage of half sectors was measured in order to determine CIN rate (Figure 3.10). The the rate of CF loss during the first cell division after plating (as indicated by half-sectors) was used as a proxy for average CIN rate.

As a positive control, we show that treatment with 10 ug/mL radicicol increases the percentage of half-sectors by a factor of 10-fold more than the DMSO solvent control (p-value = 0.0001) (Figure 3.10). Treatment with our top hit, S2161 also significantly

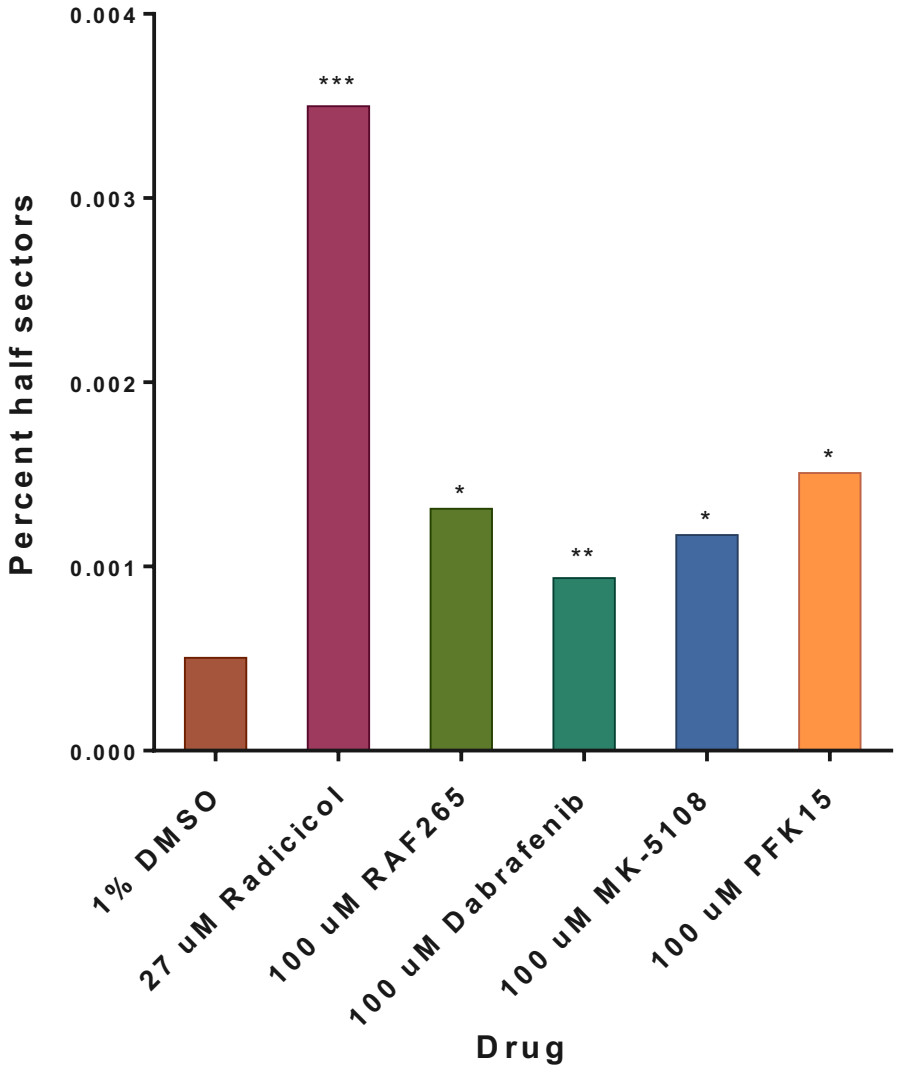

Drug	% half sectors	total colonies	half sectors	not half sectors	p-value
1% DMSO	0.000504052	75389	38	75351	
10 ug/mL Radicicol	0.003499563	3429	12	3417	0.0001
100 uM RAF265	0.00131406	7610	10	7600	0.0051
100 uM Dabrafenib	0.001170235	29054	34	29020	0.0002
100 uM MK-5108	0.000937165	44816	42	44774	0.0049
100 uM PFK15	0.001507917	3979	6	3973	0.0087

Figure 3.10: Colony sectoring assay verifies top four kinase inhibitor hits. p-values indicated are obtained from chi-square contingency tests.

increases the percentage of half sectors by 6-fold (p-value = 0.0064). As expected, the CIN fold change induced by our top hit as measured by the colony color CTF is about 10-fold less than the CIN fold change measured by the modified qCTF. The large difference is likely due to the decreased drug sensitivity of the classical CTF strain relative to the strain used for our drug screen. The classical CTF assay validated all of our top 4 hits, suggesting that our combination of qCTF assay modification, statistical analysis and false-positive exclusion methods can effectively detect and identify compounds that significantly increase chromosomal instability in yeast.

Elucidating novel pathways that contribute to CIN in budding yeast

The library used in this high throughput screen was comprised of mammalian kinase inhibitors whose targets have not been identified in budding yeast. To elucidate pathways contributing to chromosomal missegregation in yeast, yeast genes with some homology or structural similarity to each inhibitor's known mammalian targets were deleted in wildtype diploid (RLY8494) and haploid (RLY8492) qCTF strains containing the mini chromosome. The CIN rate of these deletion strains was investigated by qCTF assay in order to identify possible yeast targets of our top mammalian hits.

Two of our four hits target raf and perturb the MAPK pathway (Table 3.3), which mediates cellular response to environmental cues by coupling inputs from cell surface receptors to transcriptional regulators in the nucleus (Molina & Adjei, 2006). Components of the MAPK pathway in yeast – STE11, BMH1, PBS2, and HOG1 – were initially chosen for further investigation as drug targets and as potential mediators of chromosomal instability. STE11 is a MEKK that shares structural similarity with mammalian MAPKKKs

Inhibitor	Mammalian Targets	Yeast Homologs
RAF265	C-Raf/B-Raf/B-Raf V600E	STE11, BMH1, PBS2, HOG1
Dabrafenib	B-Raf V600E	(same as above)
MK-5108	Aurora A	IPL1
PFK15	6-phosphofructo-2-kinase (PFKFB3)	YLR345W

Table 3.3: Potential drug targets in yeast.

and acts in 3 of the 5 MAPK pathways – pheromone response, filament invasion, and high-osmolarity growth pathways (Herskowitz, 1995; Gustin, Albertyn, Alexander, & Davenport, 1998). It was chosen as a likely target of our raf inhibitors because of its extensive involvement in the MAPK pathway and homology with mammalian MAPKKKs. BMH1 is one of two yeast isoforms of 14-3-3 proteins, a family of highly conserved proteins involved in various cellular functions including vesicle trafficking, protein localization, cytokinesis, and stress response (van Heusden & Yde Steensma, Yeast 14-3-3 proteins, 2006). The first 250 residues of Bmh1p in particular share 91% identity with the mammalian 14-3-3ε isoform, which is crucial for mitotic timing in drosophila (van Heusden & Yde Steensma, Yeast 14-3-3 proteins, 2006; Hermeking, 2003). The yeast MEK and MAPK homologs, PBS2 and HOG1, respectively, are components of the MAPK's HOG pathway (Herskowitz, 1995). PBS2 is a scaffold protein that binds both STE11 and HOG1, and aids in signal transduction from osmolarity-sensitive receptors to HOG1 (Lodish, 2000). Furthermore, PBS2 activates HOG1, which regulates the expression of stress response genes induced by increased osmolarity (Gustin, Albertyn, Alexander, &

Davenport, 1998). Because the MAPK pathway is extensive, these four genes were chosen as an initial starting point and we expect to expand our current list to components in other MAPK pathways. We previously observed that the deletion of genes regulating drug efflux pumps produces a 2-fold elevation in CIN. As a result, we are interested in investigating components in the MAPK's cell wall integrity pathway in the future.

Our third hit inhibits an aurora kinase, for which only one exists in yeast. Discovered in a screen for mutants with abnormal chromosome segregation, IPL1 (increase-in-ploidy 1) aids in correcting improper chromosome-spindle associations by destabilizing the attachments between microtubules and kinetochores through phoshporylation (Chan & Botstein, 1993; Musacchio & Salmon, 2007). Studies suggest that destabilization may be driven by the lack of tension at the kinetochore during sister chromatid separation (Musacchio & Salmon, 2007). Destabilization of microtubule-kinetochore attachments by IPL1 generates unattached kinetochores, activating the spindle assembly checkpoint and allowing the cell sufficient time to correct mitotic errors (Musacchio & Salmon, 2007).

Our final hit targets the AMPK signaling pathway and inhibits a phosphofructo-kinase, PFKFB3, that produces an activator of glycolysis. YLR345W is a 6-phosphofructose-2-kinase enzyme that is predicted to synthesize fructose 2,6-bisphosphate (UniProt Consortium, 2017). Although YLR345W is an uncharacterized ORF, the p arm of YLR345W is similar in sequence to that of the mammalian 6-phosphofructo-2-kinase/fructose-2,6-bisphosphate enzymes – the closest relative being PFKFB4 in rats (BLAST E-value = 5×10^{-4}) (Zaim, Speina, & Kierzek, 2005). Interestingly, studies have shown that YLR345W links stress-induced glucose metabolism and DNA damage

response through a DNA-binding protein, CRT1 (Zaim, Speina, & Kierzek, 2005). However, whether YLR345W plays a role in inducing chromosome missegregation is unknown.

In order to further elucidate the pathways by which these inhibitors elevate CIN in yeast, homozygous and heterozygous deletion mutants were generated for each of the yeast non-essential genes, STE11, BMH1, PBS2, HOG1, and YLR345W. Of the heterozygous deletions, HOG1 was found to significantly elevate CIN by a median of 1.60-fold (Figure 3.11). This increase in CIN may be explained by HOG1's role in mediating cell cycle arrest. HOG1 homozygous deletion mutants will be tested in order to elucidate how these cells respond to increases in extracellular osmolarity and its implications in maintaining chromosomal segregation fidelity (data pending).

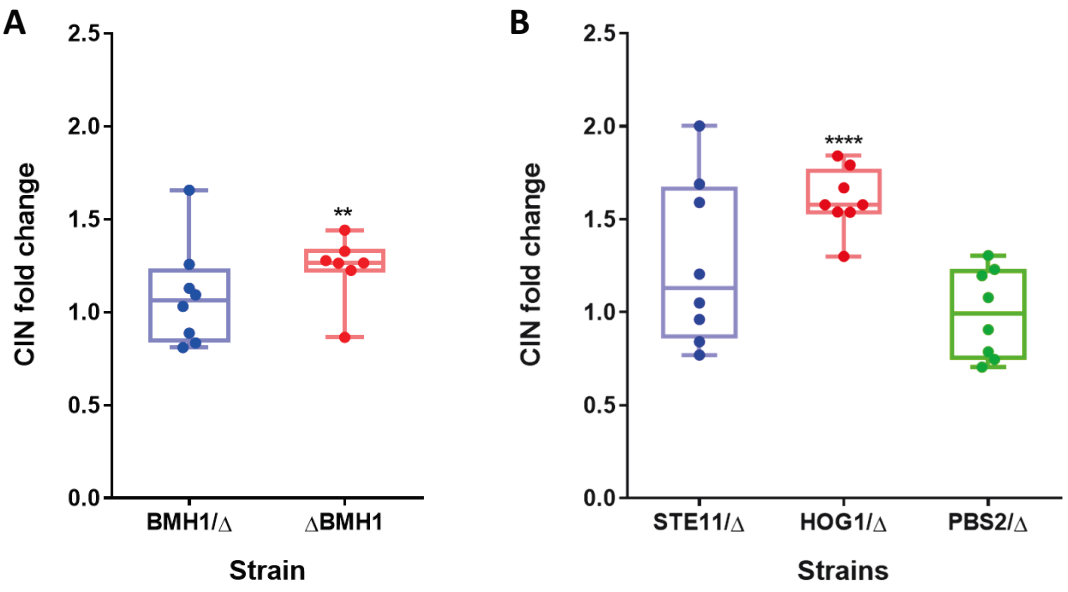

Figure 3.11: Heterozygous and homozygous deletions of MAPK components suggest that HOG1 and BMH1 may be potential mediators of chromosomal instability. Heterozygous HOG1 deletion produced a significant 1.6-fold increase in CIN ($p<0.0001$) and homozygous deletion of BMH1 produced a 1.27-fold elevation in CIN ($p = 0.0071$) (all samples were untreated). Boxplots are depicted with median fold change represented by the middle bars and individual dots representing fold change observed in each of the biological replicates. Other homozygous deletion mutants are pending.

To observe more exaggerated CIN phenotypes, we individually deleted each non-essential gene in a haploid qCTF strain (RLY8492). Homozygous deletion of BMH1 in a haploid background produced a 1.27-fold elevation in CIN even though no significant increase was observed in the BMH1 heterozygous deletion mutant, suggesting that one copy of BMH1 is sufficient to maintain chromosome transmission fidelity (Figure 3.11). To provide further evidence that BMH1 may be a drug target, the BMH1 homozygous deletion mutant will be treated with either RAF265 or dabrafenib and tested using the qCTF assay. Elevations in CIN should not be observed if BMH1 is a target. The increases in CIN observed in the homozygous BMH1 deletion mutant is supported by a recent study, which demonstrated that BMH1 is necessary for symmetric localization of spindle pole bodies in yeast (Caydasi, Micoogullari, Kurtulmus, Palani, & Pereira, 2014). Furthermore, the same study proposed BMH1 as an additional component of the SPOC (spindle position checkpoint) that ensures the proper alignment of the the mitotic spindle along the poles prior to cell division (Caydasi, Micoogullari, Kurtulmus, Palani, & Pereira, 2014).

The non-essential gene, YLR345W, was deleted in a diploid and haploid background to test its potential as a target of PFK15. Significant increases in CIN were not observed, suggesting that this gene does not play a critical role in chromosome partitioning (Figure 3.12). Other yeast 6-phoshpofructo-2-kinases enzymes, such as PFK26 and PFK27, will be tested in the future.

To identify the yeast target of the Aurora A inhibitor, MK-5108, heterozygous IPL1 deletion mutants were generated in a wildtype diploid qCTF background since IPL1 is an essential gene. Interestingly, increases in CIN were not observed upon heterozygous deletion of IPL1 (Figure 3.13). We speculated that one copy of IPL1 was sufficient to

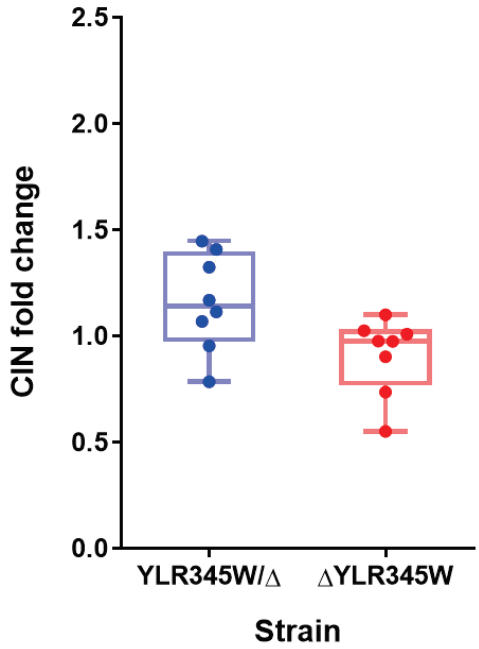

Figure 3.12: YLR345W is not required for proper chromosome segregation. Both YLR345W heterozygous and homozygous deletion mutants do not produce significant elevations in CIN.

maintain chromosome transmission fidelity in yeast and further reductions in IPL1 expression would increase CIN. The IPL1 heterozygous deletion mutant was then treated with different concentrations of MK-5108 to test if additional reduction of functional IPL1 would significantly increase CIN. Treatment with 100 uM MK-5108 increased CIN in the IPL1 deletion mutant by a median of 1.50-fold ($p= 0.0034$) more than the wildtype under the same treatment conditions, suggesting that the mammalian aurora A inhibitor may be interacting with its homolog in yeast. Increases in CIN were not observed between the heterozygous deletion mutant and wildtype under other treatment conditions (10 uM MK-5108, DMSO treatment, or untreated). Moreover, significant 1.37-fold increases were also observed between heterozygous IPL1 deletion mutants treated with 100 uM inhibitor and

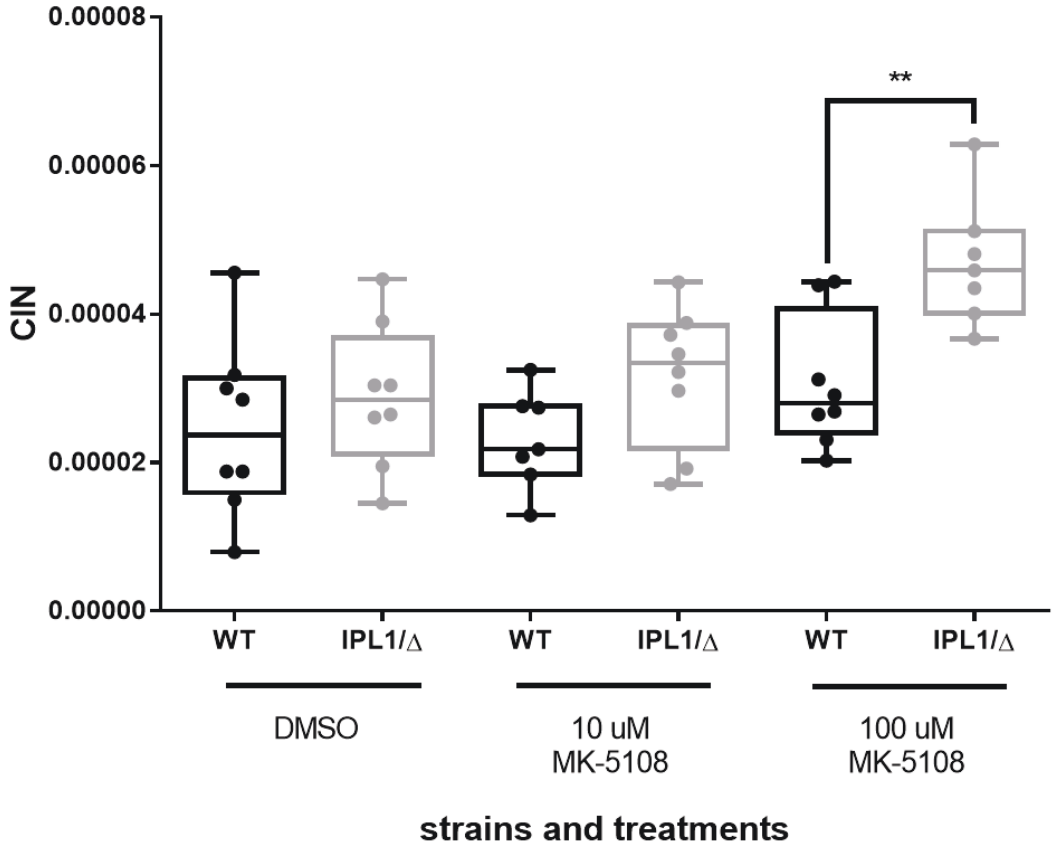

Figure 3.13: CIN of heterozygous IPL1 deletion mutant treated with aurora A kinase inhibitor, MK-5108. Mutants treated with 100 uM inhibitor show a significant 1.50-fold median elevation in CIN relative to wildtype strains treated with the same concentration of inhibitor ($p = 0.0034$). Treatment of the IPL1 mutant with 100 uM inhibitor also produces a significant 1.61-fold median increase in CIN relative to treatment of the mutant with the DMSO control ($p= 0.0023$) (not shown). A significant difference was also observed when the IPL1 mutant was treated with 10 uM and 100 uM inhibitor ($p = 0.0061$) (not shown).

10 uM inhibitor, indicating that high drug dosage is required to elicit detectable responses in wildtype yeast in order to account for robust drug efflux. Taken together, this data suggests that MK-5108 may target IPL1 in yeast, and corroborates literature demonstrating that reductions in functional IPL1 increases chromosomal instability (Chan & Botstein, 1993). Additional biochemical assays demonstrating IPL1 binding to the inhibitor must be performed in order to definitively show that MK-5108 targets IPL1.

Chapter 4: Conclusions

Summary

In this study, we identify four kinase inhibitors that significantly increase chromosome missegregation and propose pathways that may be implicated in maintaining faithful chromosome partitioning. We demonstrate the versatility of the qCTF assay by adapting it for high throughput screening through increasing drug sensitivity and weakening the mitotic checkpoint. We then developed a pipeline for cost-effective screening, false positive exclusion, hit verification, and identification of aneugens in budding yeast. During the hit identification process, we encountered and addressed a weakness of many fluorescence-based assays. Additional phenotypic validation assays and cell sorting experiments showed that interference from colored drugs may generate false positives; however, these complications could be resolved by examining GFP profiles, using additional channels during flow cytometry, and/or staining with a viability dye. From our identified hits, we came up with possible drug targets based on inhibitors' known mammalian targets to identify novel genetic modulators of CIN. Finally, we propose that components of the MAPK pathway, HOG1 and BMH1, may be involved in maintaining faithful chromosome segregation.

Future directions

In the future, we aim to improve the current qCTF assay by increasing its dynamic range and accuracy in measuring CIN. We propose to continue challenging the limits of the dynamic range by increasing the basal CIN rate of the adapted qCTF strain. The capacity to observe significant reductions in MC loss rate will allow us to identify genome protective compounds that decrease CIN and may prevent cancer development.

Furthermore, the mathematical model used in this study to calculate CIN assumed equal doubling times between MC+ and MC- populations. However, 27 kinase inhibitors in our screen produced negative CIN values, suggesting that fitness differences exist between the two populations. To account for this competition, we are developing a calibration strain with a different reporter (RFP) that matches the genotype and karyotype of MC- cells. By tracking the growth of the calibration strain, we can predict the growth of the MC- population and correct for differences in doubling times to obtain more accurate CIN measurements (refer to Zhu, et al., 2015 for the mathematical model and related equations).

Additionally, to study how our kinase inhibitor hits affect chromosome partitioning in more complex systems, we aim to investigate these hits in mammalian cell lines by performing chromosome spreads and live-cell imaging experiments. Observing chromosome missegregation events in real time may provide hints as to how each hit interferes with the segregation machinery. Finally, we hope to extend the current high throughput pipeline to larger libraries of FDA-approved compounds and natural products to identify genome protective compounds, repurpose existing drugs, and/or caution against chromosomal instability as a potential side effect of existing therapeutics.

Bibliography

Amin, M., Minton, S. E., LoRusso, P. M., Krishnamurthi, S. S., Pickett, C. A., Lunceford, J., & Trull, L. (2016). A phase I study of MK-5108, an oral aurora a kinase inhibitor, administered both as monotherapy and in combination with docetaxel, in patients with advanced or refractory solid tumors. *Investigational new drugs, 34*(1), 84-95.

Anand, S., Penrhyn-Lowe, S., & Venkitaraman, A. R. (2003). AURORA-A amplification overrides the mitotic spindle assembly checkpoint, inducing resistance to Taxol. *Cancer cell, 3*(1), 51-62.

Array BioPharma. (2016, February). *MEK162 and RAF265 in Adult Patients With Advanced Solid Tumors Harboring RAS or BRAFV600E Mutations*. Retrieved from Clinicaltrials.gov: https://clinicaltrials-gov.proxy1.library.jhu.edu/ct2/show/NCT01352273?term=raf265&rank=2

Atsumi, T., Chesney, J., Metz, C., Leng, L., Donnelly, S., Makita, Z., & Bucala, R. (2002). High expression of inducible 6-phosphofructo-2-kinase/fructose-2, 6-bisphosphatase (iPFK-2; PFKFB3) in human cancers. *Cancer research, 62*(20), 5881-5887.

Bakhoum, S. F., & Compton, D. A. (2012). Chromosomal instability and cancer: a complex relationship with therapeutic potential. *The Journal of clinical investigation, 122*(4), 1138-1143.

Bakhoum, S. F., Kabeche, L., Murnane, J. P., Zaki, B. I., & Compton, D. A. (2014). DNA-damage response during mitosis induces whole-chromosome missegregation. *Cancer discovery, 4*(11), 1281-1289.

Bakhoum, S. F., Thompson, S. L., Manning, A. L., & Compton, D. A. (2009). Genome stability is ensured by temporal control of kinetochore–microtubule dynamics. *Nature cell biology, 11*(1), 27-35.

Balzi, E., & Goffeau, A. (1995). Yeast multidrug resistance: the PDR network. *Journal of bioenergetics and biomembranes,, 27*(1), 71-76.

Barber, T. D. (2008). Chromatid cohesion defects may underlie chromosome instability in human colorectal cancers. . *Proceedings of the National Academy of Sciences, 105*(9), 3443-3448.

Cahill, D. P., Kinzler, K. W., Vogelstein, B., & Lengauer, C. (199). Genetic instability and darwinian selection in tumours. *Trends in cell biology, 9*(12), M57-M60.

Caydasi, A. K., Micoogullari, Y., Kurtulmus, B., Palani, S., & Pereira, G. (2014). The 14-3-3 protein Bmh1 functions in the spindle position checkpoint by breaking Bfa1 asymmetry at yeast centrosomes. *Molecular biology of the cell, 25*(14), 2143-2151.

Chan, C. S., & Botstein, D. (1993). Isolation and characterization of chromosome-gain and increase-in-ploidy mutants in yeast. *Genetics, 135*(3), 677-691.

Chen, G. B. (2012). Hsp90 stress potentiates rapid cellular adaptation through induction of aneuploidy. *Nature, 482*(7384), 246-250.

Clem, B. F., O'Neal, J., Tapolsky, G., Clem, A. L., Imbert-Fernandez, Y., Kerr, D. A., & Telang, S. (2013). Targeting 6-phosphofructo-2-kinase (PFKFB3) as a therapeutic strategy against cancer. *Molecular cancer therapeutics, 12*(8), 1461-1470.

Dunstan, H. M., Ludlow, C., Goehle, S., Cronk, M., Szankasi, P., Evans, D. R., & Lamb, J. R. (2002). Cell-based assays for identification of novel double-strand break-inducing agents. *Journal of the National Cancer Institute, 94*(2), 88-94.

Emter, R., Heese-Peck, A., & Kralli, A. (2002). ERG6 and PDR5 regulate small lipophilic drug accumulation in yeast cells via distinct mechanisms. *FEBS letters, 521*(1-3), 57-61.

Ernst, R., Klemm, R., Schmitt, L., & Kuchler, K. (2005). Yeast ATP-Binding Cassette Transporters: Cellular Cleaning Pumps. *Methods in enzymology, 400*, 460-484.

Escoté, X., Zapater, M., Clotet, J., & Posas, F. (2004). Hog1 mediates cell-cycle arrest in G1 phase by the dual targeting of Sic1. *Nature Cell Biology, 6*(10), 997-1002.

Faesen, A. C., Thanasoula, M., M. S., Breit, C., Müller, F., Van Gerwen, S., . . . Musacchio, A. (2017). Basis of catalytic assembly of the mitotic checkpoint complex. *Nature, 542*(7642), 498-502.

GlaxoSmithKline. (2014). *Tafinlar.* Researh Triangle Park: FDA.

Gustin, M. C., Albertyn, J., Alexander, M., & Davenport, K. (1998). MAP Kinase Pathways in the YeastSaccharomyces cerevisiae. *Microbiology and Molecular biology reviews, 62*(4), 1264-1300.

Hauschild, A., Grob, J. J., Demidov, L. V., Jouary, T., Gutzmer, R., Millward, M., & Martín-Algarra, S. (2012). Dabrafenib in BRAF-mutated metastatic melanoma: a multicentre, open-label, phase 3 randomised controlled trial. *The Lancet, 380*(9839), 358-365.

Hermeking, H. (2003). The 14-3-3 cancer connection. *Nature Reviews Cancer, 3*(12), 931-943.

Herskowitz, I. (1995). MAP kinase pathways in yeast: for mating and more. *Cell, 80*(2), 187-197.

Holderfield, M., Nagel, T. E., & Stuart, D. D. (2014). Mechanism and consequences of RAF kinase activation by small-molecule inhibitors. *British journal of cancer, 111*(4), 640-645.

Holland, A. J., & Cleveland, D. W. (2009). Boveri revisited: chromosomal instability, aneuploidy and tumorigenesis. *Nature reviews Molecular cell biology, 10*(7), 478-487.

Janssen, A., Kops, G. J., & Medema, R. H. (2009). Elevating the frequency of chromosome mis-segregation as a strategy to kill tumor cells. *Proceedings of the National Academy of Sciences, 106*(45), 19108-19113.

Jin, N., Jiang, T., Rosen, D. M., Nelkin, B. D., & Ball, D. W. (2011). Synergistic action of a RAF inhibitor and a dual PI3K/mTOR inhibitor in thyroid cancer. *Clinical Cancer Research, 17*(20), 6482-6489.

Kops, G. J., Weaver, B. A., & Cleveland, D. W. (2005). On the road to cancer: aneuploidy and the mitotic checkpoint. *Nature Reviews Cancer, 5*(10), 773-785.

Lara-Gonzalez, P. W. (2012). The spindle assembly checkpoint. *Current biology, 22*(22), R966-R980.

Lodish, H. B. (2000). MAP Kinase Pathways. In H. B. Lodish, *Molecular Cell Biology.* New York: W. H. Freeman.

Marumoto, T., Honda, S., Hara, T., Nitta, M., Hirota, T., Kohmura, E., & Saya, H. (2003). Aurora-A kinase maintains the fidelity of early and late mitotic events in HeLa cells. *Journal of Biological Chemistry, 278*(51), 51786-51795.

Matsuura, S., Matsumoto, Y., Morishima, K. I., Izumi, H., Matsumoto, H., Ito, E., & ... & Hama, S. (2006). Monoallelic BUB1B mutations and defective mitotic-spindle checkpoint in seven families with premature chromatid separation (PCS) syndrome. *American journal of medical genetics Part A, 140*(4), 358-367.

McCammon, M. T., Hartmann, M. A., Bottema, C. D., & Parks, L. W. (1984). Sterol methylation in Saccharomyces cerevisiae. *Journal of bacteriology, 157*(2), 475-483.

Molina, J. R., & Adjei, A. A. (2006). The Ras/Raf/MAPK pathway. *Journal of Thoracic Oncology, 1*(1), 7-9.

Morrison, D. K. (2012). MAP kinase pathways. *Cold Spring Harbor perspectives in biology, 4*(11), a011254.

Moye-Rowley, W. S. (2003). Transcriptional control of multidrug resistance in the yeast Saccharomyces. *Progress in nucleic acid research and molecular biology, 73*, 251-279.

Mukhopadhyay, K. K. (2002). Drug Susceptibilities of Yeast Cells Are Affected by Membrane Lipid Composition. *Antimicrobial Agents and Chemotherapy, 46*(12), 3695-3705.

Mukhopadhyay, K., Kohli, A., & Prasad, R. (2002). Drug Susceptibilities of Yeast Cells Are Affected by Membrane Lipid Composition. *Antimicrobial Agents and Chemotherapy, 46*(12), 3695-3705.

Mulla, W., Zhu, J., & Li, R. (2014). Yeast: a simple model system to study complex phenomena of aneuploidy. *FEMS microbiology reviews, 38*(2), 201-212.

Musacchio, A., & Salmon, E. D. (2007). The spindle-assembly checkpoint in space and time. *Nature reviews Molecular cell biology, 8*(5), 379-393.

Nikonova, A. S., Astsaturov, I., Serebriiskii, I. G., Dunbrack, R. L., & Golemis, E. A. (2013). Aurora A kinase (AURKA) in normal and pathological cell division. *Cellular and Molecular Life Sciences, 70*(4), 661-687.

Nourani, A., Wesolowski-Louvel, M., Delaveau, T., Jacq, C., & Delahodde, A. (1997). Multiple-drug-resistance phenomenon in the yeast Saccharomyces cerevisiae: involvement of two hexose transporters. *Molecular and cellular biology, 17*(9), 5453-5460.

Perkins, E., Sun, D., Nguyen, A., Tulac, S., Francesco, M., Tavana, H., & Yeh, E. (2001). Novel inhibitors of poly (ADP-ribose) polymerase/PARP1 and PARP2 identified using a cell-based screen in yeast. *Cancer Research, 61*(10), 4175-4183.

Pharmaceuticals, Novartis. (2016, November). *A Study to Evaluate RAF265, an Oral Drug Administered to Subjects With Locally Advanced or Metastatic Melanoma (CHIR-265-MEL01)*. Retrieved from Clinicaltrials.gov: https://clinicaltrials-gov.proxy1.library.jhu.edu/show/NCT00304525

Pihan, G. A. (1998). Centrosome defects and genetic instability in malignant tumors. *Cancer research, 58*(17), 3974-3985.

R&D Systems. (2017). *Flow Cytometry Protocol for Analysis of Cell Viability using Propidium Iodide*. Retrieved from https://www.rndsystems.com/resources/protocols/flow-cytometry-protocol-analysis-cell-viability-using-propidium-iodide

Redman, R., Pohlmann, P., Kurman, M., Tapolsky, G. H., & Chesney, J. (2015). Abstract CT206: PFK-158, first-in-man and first-in-class inhibitor of PFKFB3/glycolysis:

A phase I, dose escalation, multi-center study in patients with advanced solid malignancies. *AACR Annual Meeting, 75*(15), CT206.
Sajesh, B. V. (2013). Sister chromatid cohesion defects are associated with chromosome instability in Hodgkin lymphoma cells. *BMC cancer, 13*(1), 391.
Selleckchem. (2017, Februrary). *RAF265 (CHIR-265)*. Retrieved from Selleckchem.com: http://www.selleckchem.com/products/RAF265(CHIR-265).html
Sharma, S. C. (2006). Implications of sterol structure for membrane lipid composition, fluidity and phospholipid asymmetry in Saccharomyces cerevisiae. *FEMS yeast research, 6*(7), 1047-1051.
Shimomura, T., Hasako, S., Nakatsuru, Y., Mita, T., Ichikawa, K., Kodera, T., & Miki, S. (2010). MK-5108, a highly selective Aurora-A kinase inhibitor, shows antitumor activity alone and in combination with docetaxel. *Molecular cancer therapeutics, 9*(1), 157-166.
Simon, J. A., Szankasi, P., Nguyen, D. K., Ludlow, C., Dunstan, H. M., Roberts, C. J., . . . Friend, S. H. (2000). Differential toxicities of anticancer agents among DNA repair and checkpoint mutants of Saccharomyces cerevisiae. *Cancer Research, 60*(2), 328-333.
Spencer, F., Gerring, S. L., Connelly, C., & Hieter, P. (1990). Mitotic chromosome transmission fidelity mutants in Saccharomyces cerevisiae. *Genetics, 124*(2), 237-249.
Stirling, P. C., Crisp, M. J., Basrai, M. A., Tucker, C. M., Dunham, M. J., Spencer, F. A., & Hieter, P. (2012). Mutability and mutational spectrum of chromosome transmission fidelity genes. *Chromosoma, 121*(3), 263-275.
Tanaka, K., & Hirota, T. (2016). Chromosomal instability: a common feature and a therapeutic target of cancer. *Biochimica et Biophysica Acta (BBA)-Reviews on Cancer, 1866*(1), 64-75.
Thompson, S. L. (2008). Examining the link between chromosomal instability and aneuploidy in human cells. *J Cell Biol,, 180*(4), 665-672.
Thompson, S. L., Bakhoum, S. F., & Compton, D. A. (2010). Mechanisms of chromosomal instability. *Current biology, 20*(6), R285-R295.
UniProt Consortium. (2017). *Q06137 (YL345_YEAST)*. Retrieved from http://www.uniprot.org/uniprot/Q06137
van Heusden, G. P., & Yde Steensma, H. (2006). Yeast 14-3-3 proteins. *Yeast, 23*(3), 159-171.
van Heusden, G. P., & Yde Steensma, H. (2006). Yeast 14-3-3 proteins. *Yeast,, 23*(3), 159-171.
Vandeputte, P. F. (2011). Antifungal resistance and new strategies to control fungal infections. *International journal of microbiology*, 2012.
Vandeputte, P., Ferrari, S., & Coste, A. T. (2011). Antifungal resistance and new strategies to control fungal infections. *International journal of microbiology*, 2012.
Weaver, B. A., & Cleveland, D. W. (2006). Does aneuploidy cause cancer? *Current opinion in cell biology, 18*(6), 658-667.
Williams, T. E., Subramanian, S., Verhagen, J., McBride, C. M., Costales, A., Sung, L., & Levine, B. (2015). Discovery of RAF265: A Potent mut-B-RAF Inhibitor for

the Treatment of Metastatic Melanoma. *ACS medicinal chemistry letters, 6*(9), 961.

Yaakov, G., Duch, A., García-Rubio, M., Clotet, J., Jimenez, J., Aguilera, A., & Posas, F. (2009). The stress-activated protein kinase Hog1 mediates S phase delay in response to osmostress. *Molecular biology of the cell, 20*(15), 3572-3582.

Yalcin, A., Clem, B. F., Imbert-Fernandez, Y., Ozcan, S. C., Peker, S., O'neal, J., & Chesney, J. (2014). 6-Phosphofructo-2-kinase (PFKFB3) promotes cell cycle progression and suppresses apoptosis via Cdk1-mediated phosphorylation of p27. *Cell death & disease, 5*(7), e1337.

Yuen, K. W., Warren, C. D., Chen, O., Kwok, T., Hieter, P., & Spencer, F. A. (2007). Systematic genome instability screens in yeast and their potential relevance to cancer. *Proceedings of the National Academy of Sciences, 104*(10), 3925-3930.

Zaim, J. S. (2005). Identification of new genes regulated by the Crt1 transcription factor, an effector of the DNA damage checkpoint pathway in Saccharomyces cerevisiae. *Journal of Biological Chemistry, 280*(1), 28-37.

Zaim, J., Speina, E., & Kierzek, A. M. (2005). Identification of new genes regulated by the Crt1 transcription factor, an effector of the DNA damage checkpoint pathway in Saccharomyces cerevisiae. *Journal of Biological Chemistry, 280*(1), 28-37.

Zhang, W., & Liu, H. T. (2002). MAPK signal pathways in the regulation of cell proliferation in mammalian cells. *Cell research, 12*(1), 9-18.

Zhu, J., Heinecke, D., Mulla, W. A., Bradford, W. D., Rubinstein, B., Box, A., . . . Li, R. (2015). Single-cell based quantitative assay of chromosome transmission fidelity. *G3: Genes| Genomes| Genetics, 5*(6), 1043-1056.

Vivian Yeong

(856)-359-5617 | vyeong14@gmail.com

EDUCATION

Johns Hopkins University
Baltimore, Maryland **August 2015 - Present**
M.S.E Candidate in Chemical and Biomolecular Engineering
Coursework: Polymer chemistry and biology, supramolecular nanomedicine, design of bimolecular systems, transport phenomena, metabolic systems biotechnology, thermodynamics and kinetics
Master's thesis: High throughput assessment of kinase inhibitors in Saccharomyces cerevisiae identifies aneugenic compounds

Harvard University
Cambridge, Massachusetts **September 2010 - May 2014**
Honors B.A. in Molecular and Cellular Biology
Secondary Field in Mathematical Sciences
Coursework: Molecular biology, therapeutics, mathematical biology, organic chemistry
Thesis: Engineering a Light-Responsive Circadian Clock

Chinese University of Hong Kong
Shatin, Hong Kong **June 2011 - August 2011**
Study Abroad, International Summer Student
Coursework: Chinese medicinal practice and history

WORK EXPERIENCE

Johns Hopkins University Department of Chemical and Biomolecular Engineering
Baltimore, Maryland **January 2016 - Present**
Master's Thesis Research, Li lab

- Conducted a high throughput screen to identify compounds that elevate or mitigate chromosomal instability in *Saccharomyces cerevisiae* and to elucidate molecular pathways that contribute to chromosomal missegregation.
- Improved a reporter/repressor system for detecting chromosomal instability in *Saccharomyces cerevisiae*.

The Learning Lab
Singapore, Singapore **July 2014 - May 2015**
Specialist Teaching Associate and Curriculum Management

- Provided after school enrichment services in math, biology, chemistry, and physics to secondary school students. Worked with both parents and students to establish goals and provide individualized learning experiences.
- Collaborated with a team to design a chemistry curriculum for upper level secondary school students.

Harvard University Department of Systems Biology
Cambridge, Massachusetts **October 2012 - May 2014**
Thesis Research

- Genetically engineered *E. coli* to express components of the cyanobacterial Kai clock, optimized the expression levels of each clock component by assessing the behavior of the clock under various promoters, and performed Western blots to observe oscillations.
- Demonstrated that the synthetic clock can be controlled by various environmental inputs, including chemical inducers and specific wavelengths of light.

Harvard University Department of Evolutionary Biology
Cambridge, Massachusetts **May 2011 - May 2012**
Research Assistant

- Investigated the mechanistic differences and evolutionary pressures driving the discrepancy in mating frequencies between two strains of C. elegans by examining the contributions of chemosensory and self-sperm regulating genes to aversive mating behaviors.

EXTRA-CURRICULARS

Harvard College Biotechnology Association
Cambridge, Massachusetts **September 2012 - May 2014**
Director of Relations and Outreach

- Managed a relatively new student organization focused on biotechnology and career exploration opportunities for undergraduates with diverse academic interests ranging from global health to computer science.
- Organized collaborations with other student groups, discussion panels, biotech information sessions, and ask-the-investigator dinners.

SKILLS/ INTERESTS

Programming: Statistical packages (Excel, Stata); some mathematical scripting and modeling (Mathematica, LaTeX, MATLAB, Python); software packages (Microsoft Office Suite, GraphPad, SnapGene).

Laboratory skills: high throughput screening; liquid handling systems; flow cytometry; genome walking; *Saccharomyces cerevisiae* genetics; tetrad dissections; replica plating; yeast mating; yeast cell synchrony; yeast cultures and transformations; mammalian culture; MTT assay; karyotyping; DNA content analysis; Western blots; chemical induction; Gibson assembly; molecular cloning; DNA extraction and purification, sequencing and analysis; gel electrophoresis; bacterial cultures and transformations; PCR; *C. elegans* mating assays.

Interests: bioactive hydrogels; synthetic biology; drug delivery; high throughput screening; therapeutics; violin performance; dance; traveling

PROFESSIONAL SOCIETIES

American Society for Cell Biology (2016)

PUBLICATIONS

Chen, A. H., Lubkowicz, D., **Yeong, V.**, Chang, R. L., and Silver, P. A. (2015). Transplantability of a circadian clock to a noncircadian organism. *Science advances, 1*(5).

POSTER PRESENTATIONS

Institute for Basic Biomedical Sciences Symposium (2016)
Synberc Spring Symposium (2014)
Harvard Systems Biology Department Retreat (2014)
Synberc Fall Symposium (2013)
Wyss Institute Retreat (2013)
Microbial Sciences Initiative Summer Undergraduate Research Symposium (2013)

AWARDS

Johns Hopkins University,
Chemical and Biomolecular Engineering Master's Essay Scholarship (2016)
Howard Hughes Medical Institute Travel Award (2014)
Howard Hughes Medical Institute Interdisciplinary Undergraduate Fellow (2013)
Microbial Sciences Initiative Undergraduate Summer Research Fellowship (2013)
Harvard College Research Program (2013)